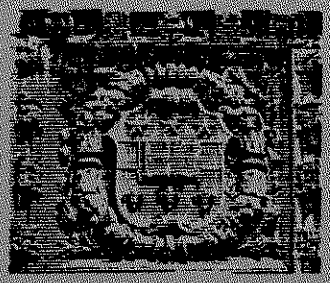

WASHINGTON UNIVERSITY

SCHOOL OF ENGINEERING AND APPLIED SCIENCE

CHEMICAL REACTION ENGINEERING LABORATORY

REPORT FOR THE PERIOD

JANUARY 1, 1977 - JUNE 1, 1978

WASHINGTON UNIVERSITY / ST. LOUIS / MISSOURI 63130

Report

January, 1977 - June, 1978

CHEMICAL REACTION ENGINEERING LABORATORY

Department of Chemical Engineering

Washington University

St. Louis, Missouri 63130

Prepared by:

Dr. M. P. Duduković
Associate Professor
and
Director
Chemical Reaction Engineering Laboratory

TABLE OF CONTENTS

INTRODUCTION

This report covers the major developments in the Chemical Reaction Engineering Laboratory (CREL) for the period January 1, 1977, through May 31, 1978.

The work in CREL has been concentrated on two major areas during the past year and a half. These areas are: gas-solid noncatalytic reactions and multiphase reactors. In the area of gas-solid noncatalytic reactions the emphasis was on modelling and experimental study of systems where the change in solid structure caused by reaction affects the further progress of reaction. In the area of multiphase reactors, catalyst effectiveness and contacting efficiency in trickle-bed reactors and gas holdup and liquid recirculation in gas-lift reactors were studied. The summary of all the projects which were completed, are in progress or in planning stage is given in Table I.

During the past period, a viable operation of the Laboratory was maintained. Three new NSF grants were received in addition to the two previous ones, as well as continued financial support from Alcoa, Amoco Oil, and Monsanto. Shell Development Company and Amoco Chemicals have also decided to join the laboratory which was most gratifying. The continued industrial interest is especially appreciated. The Industrial Laboratory advisors: Dr. K. Robinson (Amoco Oil), S. P. Ho (Amoco Chemicals), A. Pearson (Alcoa), R. Lee (Monsanto), R. Penquite (Monsanto), C. Barkelew (Shell), and other industrial consultants provided invaluable assistance in discussing various research projects.

One doctoral student (H. Lamba) completed his dissertation during the past year in the Laboratory. Currently, six (6) graduate students are working in the Laboratory. In addition, a number of undergraduates (freshmen through seniors) participated in the research activities. Three of these students were sponsored by the NSF undergraduate research participation fund each summer.

The Laboratory staff was active in the reaction engineering area also outside Washington University. Dr. M. Duduković presented a paper at the 5th International Symposium on Chemical Reaction Engineering in Houston, Texas, in March, 1978. He also gave seminars at Argonne National Laboratory and at Vanderbilt University. P. Mills and Y. Hsu presented two papers at the One-Day AIChE Symposium in St. Louis in April, 1978. Several papers were published and a number has been submitted for publication.

At the end, one would like to emphasize that considerable progress has been made on all research projects and that we expect further accomplishments during this year. All the activities are focused in the two major areas mentioned above. Further research efforts are planned exclusively in these areas provided adequate funding can be secured.

TABLE I

Active Projects in the Chemical Reaction Engineering Laboratory January, 1977 - present

AREA I: GAS-SOLID NONCATALYTIC REACTIONS

Project	Funding	Investigators	Major Results, Publications and Presentations
1. Gas-Solid Noncatalytic Reactions Relevance: All experimental investigations and parameter estimations in gas-solid noncatalytic reactions	NSF and Alcoa	M. P. Duduković H. S. Lamba O. Garza-Garza	a) Formulation of new highly efficient computational techniques for solution of models for gas-solid reactions. b) Experimental and theoretical confirmation of the large effect of change in structure on reaction rates of solid particles. 1. M. P. Duduković and H. S. Lamba, "Solution of Moving Boundary Problems for Gas-Solid Noncatalytic Reactions by Orthogonal Collocation," Chem. Eng. Science, 33, 303-314 (1978). 2. M. P. Duduković and H. S. Lamba, "A Zone Model for Reactions of Solid Particles with Strongly Adsorbing Species," Chem. Eng. Science, 33, 471-478 (1978). 3. H. S. Lamba and M. P. Duduković, "A New Technique for Solution of Models for Reaction of Solid Solution of Solid Particles and for Parallel Catalyst Deactivation," The Chem. Eng. Journal, to appear in 1978. 4. One paper in preparation.

TABLE I (Cont.)

AREA I: GAS-SOLID NONCATALYTIC REACTIONS

Project	Funding	Investigators	Major Results, Publications and Presentations
2. Fluorine Recovery From the Waste Products of the Phosphate Fertilizer Industry	NSF and Alcoa	M. P. Duduković H. S. Lamba	Use of waste products silicofluorides to fluorinate halogenated hydrocarbons. Feasibility of the reactions to make freons proven. Kinetic data obtained for reactions of Ba Si F_6 with CCl_4, thermal decomposition of Ba Si F_6 and for the reaction of Ba F_2 with CCl_4. The effect of change in structure of the solid on reaction examined and quantified. 1. H. S. Lamba, "Experimental Study and Modelling of Noncatalytic Gas-Solid Reactions of Silicofluorides," D.Sc. Thesis, Washington University, St. Louis, August, 1978. 2. Papers in preparation.
3. Effect of change on Solid Structure on Reaction Rates of Solid Particles	NSF	M. P. Duduković O. Garza-Garza	Project in planning stage. The goal is to interpret properly the effect of change in molar volumes of the solid on transport coefficients and reaction rates in isothermal systems. After this is done the effect of sintering is to be studied also.

TABLE (Cont.)

AREA II: MULTIPHASE REACTORS

Project	Funding	Investigators	Major Results, Publications and Presentations
1. Liquid-Solid Contacting and Catalyst Effectiveness in Trickle-Bed Reactors Relevance: Desulfurization of petroleum and coal derived liquids. Trickle-bed scale-up and design.	NSF Amoco Oil Shell Development	M. P. Dudukovic P. L. Mills	a) Complete development of an experimental set-up for tracer studies to measure contacting by using non-adsorbable and adsorbable tracers. Automation of data acquisition and processing. b) Mathematical modelling and evaluation of the effect of particle scale incomplete contacting. 1. M. P. Dudukovic, "Catalyst Effectiveness Factor and Contacting Efficiency in Trickle-Bed Reactors," AIChE J., 23(6), 940-943 (1977). 2. M. P. Dudukovic and P. L. Mills, "Catalyst Effectiveness Factor in Trickle-Bed Reactors," 5th International Symposium on Chemical Reaction Engineering, Houston, Texas, March, 1978, ACS Symposium Series 65, 387-399 (1978). 3. P. L. Mills and M. P. Dudukovic, "The Effect of Partial Wetting on Catalyst Effectiveness in Trickle-Bed Reactors," One-Day AIChE Symposium, St. Louis, August 4, 1978. 4. P. L. Mills and M. P. Dudukovic, "A Dual-Series Solution for the Effectiveness Factor of Partially Wetted Catalysts in Trickle-Bed Reactors," submitted for publication. 5. Papers in preparation.

TABLE I (Cont.)

AREA II: MULTIPHASE REACTORS

Project	Funding	Investigators	Major Results, Publications and Presentations
2. Models for Trickle-Bed Reactors Relevance: Scale-up and design of trickle-bed reactors	NSF Amoco Oil Shell Development	M. P. Dudukovic P. L. Mills A. A. Elhishnawi H. C. Kao G. Maxwell	Search for feasible model reactions continues. One example of nonvolatile liquid reactant and one of highly volatile liquid reactant is sought. The reactions should proceed at moderate temperatures and atmospheric pressure. The goal is to determine all kinetic data independently and compare the predicted performance of a trickle-bed designed for high conversion with actual conversion obtained. Project is in progress.
3. Gas-Lift Recirculation Reactor Relevance: Reactor design for hydrogenation and oxidations in chemical industry	Amoco Chemicals Monsanto	M. P. Dudukovic Y. C. Hsu	Development of a method based on circulation balance for prediction of liquid recirculation rates. Development of a gas-holdup correlation at high liquid velocities and a criterion for the change in flow regime. 1. Y. C. Hsu and M. P. Dudukovic, "Prediction of Gas Holdup and Liquid Recirculation RAtes in Gas-Lift Recycle Reactor," One Day AichE Symposium, St. Louis, August, 1978.

TABLE I (Cont.)

AREA II: MULTIPHASE REACTORS

Project	Funding	Investigators	Major Results, Publications and Presentations
4. Backmixing in Bubble Columns Relevance: Identification of the extent of gas and liquid backmixing.	Monsanto and Departmental	M. P. Dudukovic J. R. Faber	Investigation of gas and liquid backmixing in bubble columns in the presence and absence of solids, baffles, and at different L/D ratios. Significant gas backmixing detected even in columns of 6" diameter. Correlations for liquid and gas backmixing presented. 1. J. R. Faber, "Axial Dispersion in Bubble Columns," M.S. Thesis, Washington University, St. Louis, June, 1977.

TABLE I (Cont.)

AREA III: OTHER STUDIES

Project	Funding	Investigators	Major Results, Publications and Presentations
1. Effect of Micromixing on Reactor Performance Relevance: Homogeneous systems with slow reactions	---	M. P. Duduković	Demonstration that micromixing may considerably affect all criteria for uniqueness of steady states and that multiple steady states may arise unexpectedly where classical theory based on maximum mixedness predicts a single steady state. 1. M. P. Duduković, "Micromixing Effects on Multiple Steady States in Stirred Tank Reactors," AIChE J., 23(3), 382-385 (1977). 2. M. P. Duduković, "Micromixing Effects on Multiple Steady States in Isothermal Chemical Reactors," Chem. Eng. Sci., 32, 985-994 (1977). 3. M. P. Duduković, "On the Generalized Recycle Model as a Model of Micromixing," Ind. Eng. Chem. Fundamentals, 16(3), 385-388 (1977).

REVIEW OF RESEARCH PROJECTS

Research efforts within CREL have been concentrated in two major areas:

I. Gas-Solid Noncatalytic Reactions,

II. Multiphase Reactors.

The overall objectives in these two areas are:

I. To develop a better understanding of complex phenomena occurring in gas-solid noncatalytic reactions and to provide guidelines and rational experiment designs for determination of important rate parameters which are necessary for proper reactor design. To account in a quantitative manner for the effect of change in solid structure during reaction on transport and rate parameters.

II. To develop more fundamental information about multiphase reactors (trickle-beds, gas-lift, bubble columns) that will be useful in scale-up and design.

A brief summary of major research accomplishments and further planned work on various projects follows.

AREA I: Gas-Solid Noncatalytic Reactions

Project 1: Gas-Solid Noncatalytic Reactions

A. Problem Definition

Reactions of solid particles play an important role in ore roasting and leaching, in coal conversion, and in a number of chemical processes. Modelling reactions of solid particles is necessary for evaluation of rate parameters from experimental data and in proper reactor design.

Our goal is to develop a comprehensive mathematical model for reaction of solid particles which relies on experimental evidence of physical phenomena. The incorporation of structural changes with reaction into the model is of major importance. Other previous attempts in this area were not successful due to a lack of efficient computational techniques. When the ratio of the maximum kinetic rate and maximum internal diffusion rate in the solid reactant is not large (i.e. when Thiele modulus is not large) shrinking core models cannot be used and diffusion with simultaneous reaction models have to be employed. These models result in a system of coupled partial differential equations which is tedious to solve by conventional finite difference methods and requires excessive computer storage and time. This fact made the use of single pellet reaction rate models in reactor design forbidding.

B. Research Accomplishments

The details of the research accomplishments are available in the papers quoted in Table I under the above project title. In summary, the following accomplishments were achieved:

1. Reduction of computational costs by two orders of magnitude for models for reaction of solid particles according to any type of diffusion and simultaneous reaction models by either:
   i) reducing the coupled system of partial differential equations by an integral transformation to a set of initial value problems either in time or in space, or
   ii) reducing the coupled system of partial differential

equations to a set of ordinary differential equations using orthogonal collocation.

2. Incorporation of the effect of structural changes in the solid on effective diffusivity in solid pellets.

C. Further Research Plans

-- incorporation of the effect of change in structure on apparent kinetic parameters by the use of changing size grain model.

-- development of approximate semianalytical solutions to be used in reactor design.

-- use of developed models in interpretation of calcium oxide sulfation reaction.

Project 2. Fluorine Recovery from the Waste Products of the Phosphate Fertilizer Industry

A. Problem Definition

The limited world wide proven reserves of cryolite and fluorspar, which are the only two naturally occurring minerals containing industrially significant amounts of fluorine are decreasing and cannot sustain the exponentially increasing production of fluorinated chemicals for an extended period. However, many man-made materials and byproducts of several industries contain considerable amounts of fluorine. Among them, silicofluorides, the waste products of the phosphate fertilizer industry, contain more fluorine than any naturally occurring mineral. Our goal was to investigate the possibilities of using silicofluorides directly as fluorinating agents.

B. Research Accomplishments

Thermal decomposition of silicofluorides and the reactions of carbon-tetrachloride with barium silicofluoride or barium fluoride were studied in a single pellet reactor. Additional experiments using B.E.T. adsorption, mercury porosimetry, x-ray diffraction, electron microscopy, etc., were performed to determine the effect of pressure under which the pellet was made and of structural changes due to reaction on these quanities.

It was demonstrated experimentally that silicofluorides which contain more fluorine than any naturally occurring mineral, can be used successfully to fluorinate halogenated hydrocarbons such as carbon tetrachloride and that solid conversions around 75% can be achieved with pellets of 1 cm. in diameter in about 90 minutes even at temperatures as low as 300°C. These reactions consist of two steps: the thermal decomposition of silicofluoride followed by the reaction of fluoride with carbontetrachloride. The kinetic and diffusion parameters were quantitatively evaluated for this second reaction for pellets of 1 cm. made at pressures between 4500 to 8000 psia giving effective diffusivities from 0.057 $\frac{2}{cm}$/s to 0.087 $\frac{2}{cm}$/s and an apparent activation energy for the rate masked by diffusional effects of 5.5 kcal/mol for the temperatures from 300° to 500°C. Due to the increase in molar volume of the solid and due to pore closure, the reaction stops short of complete conversion.

A brief research summary is given in Appendix A -- while additional details can be found in the thesis by Lamba, which is available upon request.

C. Further Research Plans

Further studies of the reaction between Ba F_2 and CCl_4 are planned. This reaction is almost ideal for investigation of the effect of change in solid structure (Ba F_2 to Ba Cl_2 transformation) on reaction rate. The heat of reaction is very low (less than 0.4 kcal/gmol) and the system can be considered isothermal. The reaction temperatures (300 - 500°C) are far below Tammann temperatures for the solids involved so that sintering effects are neglible also. The leveling off of the conversion - time curve at about 0.8 can be attributed solely to the effect of increase in molar volume of the solid. Further investigation of this phenomena is planned since no current model can match entirely the experimental conversion - time curve.

Project 3. Effect of Change in Solid Structure on Reaction Rates of Solid Particles

A. Problem Definition

In many industrially important gas-solid reactions, it is observed that solid conversion stops short of completion. The sudden slow-down in conversion - time curve (i.e. the remarkable decrease of the reaction rate) is attributed to the change in solid structure with reaction. These structural changes may be caused primarily by the difference in molar density of the solid reactant and product, by the difference in crystal structure of the solid reactant and product and by sintering effects. The final result is pore closure which makes some unreacted portions of the solid pellet inaccessible to reactant gases except via

extremely slow diffusion through the compact solid product layer. Modeling of these phenomena is important in order to be able to predict the slow-down of the rate and to assess the effect of the initial porosity and pore structure on reaction progress.

B. Research Accomplishments

The project has just been initiated. Literature survey has been completed.

C. Further Research Plans

The following model types will be examined as to their effectiveness in accounting for the effect of the change in structure:

1. A simultaneous diffusion with reaction model where the effective diffusivity varies with local porosity which in turn is a function of local conversion while the apparent rate constant is a function of local surface area which also depends on local conversion.
2. A simultaneous diffusion with reaction model where the effective diffusivity varies as above, but the rate per unit volume of the pellet is given by the rate per grain times the number of grains per unit volume of the pellet. In addition, the grain size varies with progress of reaction due to differences in molar volume of solid reactant and product.
3. A single pore model where due to the difference in molar volume of the solid reactant and product the pore mouth may close prior to reaction completion if the pore Thiele modulus is large.

4. Extension of the above models.

Test reactions suggested for experimental investigation and model evaluation are:

a) $Ba\ F_2 + CCl_4 = Ba\ Cl_2 + CCl_3F$

b) $CaO + H_2S = CaS + H_2O$

c) $CaO + SO_2 + \frac{1}{2}O_2 = Ca\ SO_4$

The first reaction can be modeled as a completely isothermal system due to very low heat of reaction. The reaction occurs at temperatures at which sintering effects are unimportant. Thus, this reaction will be a true test for the best way to model the effect of change in solid molar volume on reaction. The second reaction can be conducted at temperatures where sintering effects are negligible and will provide a test whether the model developed for the first reaction is general enough to apply to a different reaction system. At higher temperatures, additional sintering effects will be studied. The third reaction provides the test for the overall model at conditions where sintering effects are pronounced.

It is especially of interest to determine whether the same model type will hold for naturally occurring consolidated rocks such as $CaCO_3$ (thermally decomposed to CaO) and for pellets made by pelletization of powder ($Ba\ F_2$). Besides reaction studies on extensive experimental program in evaluation of effective diffusivities, pore size distribution, surface area, etc., is planned.

AREA II: Multiphase Reactors

Project 1: Liquid-Solid Contacting and Catalyst Effectiveness in Trickle-Bed Reactors

A. Problem Definition

Trickle-bed reactors represent an important class of three-phase reactors used for liquid-gas contacting in the presence of a catalyst. The use of this reactor type is widely spread in petroleum industry and shows promise for coal liquefaction and chemical processing also, provided its scale-up and design can be facilitated.

One of the most important parameters for design of trickle-bed reactors is the catalyst area that is effectively wetted by liquid (contacting efficiency). Three methods have been used to determine catalyst contacting efficiencies:

1. Measurement of dissolution rates of solid particles (benzoic acid);
2. Comparison of performance of the same catalyst in trickle-bed and basket (Carberry type) reactors;
3. Tracer methods using adsorbable and nonadsorbable tracers.

The disadvantages of the first method is that realistic liquids cannot be used and the method is not usable for testing of large scale industrial reactors. The validity of the second method has never been proven conclusively. The third method is general in nature and readily applicable to laboratory, pilot or industrial scale reactors.

Project 3: Gas-Lift Recirculation Reactor

A. Problem Definition

Gas-lift-slurry reactors represent another alternative to trickle-beds for gas-liquid contacting in the presence of the solid catalyst. This reactor configuration is very useful for operation at terminal conditions as it can be operated at large recycle ratios as a stirred tank without moving parts.

Although bubble columns with suspended slurries have been extensively investigated, almost no experimental information is available on gas-lift reactors where liquid velocity in the up-leg can be order of magnitude greater than in bubble columns. Therefore, it is of interest to determine how liquid holdup and liquid-gas mass transfer depend on liquid recirculation and solids concentration.

B. Research Accomplishments

A thorough literature survey of the work done on bubble columns and gas-lift systems has been performed. A reactor prototype has been constructed and a first series of tests with air-water system has been completed. A method for predicting liquid recirculation velocity has been developed and a correlation for gas holdup based on experimental data has been obtained. A brief summary of the first series of tests is included in Appendix C.

C. Further Research Plans

1. Testing with systems other than air-water to determine the effect of physical properties is in progress.

up more large pores (transition from Cruve I to Curve III in Figure 5) while a reaction with decrease in molar density closes up some of the major pores (transition from Curve III to Curve II in Figure 5).

Unreacted, partially reacted and reacted pellets were further characterized by using x-ray diffraction scanning electron microscopy, grain size distribution, electron microprobe analysis, B.E.T. surface area determination and quantitative chemical analysis. The details and results are given in the thesis by Lamba.

Independent measurements of effective diffusivity were performed using the steady state Wicke-Kallenbach cell and the He-N_2 binary system at room temperatures. The variation of the tortuosity factor with the pressure under which the pellet was made was determined. It was estimated that the temperature dependence of the effective diffusivity can be described by "diffusion activation energy" of 1.63 kcal/mol or by a corresponding temperature power coefficient of 1.27.

A computer program was developed to evaluate the kinetic parameters from the experimental conversion versus time curves for reaction (1). The program is based on minimization of the sum of the squares of the differences between model predicted and experimental conversions at N discrete points in time. It was shown that a model based on the second order apparent reaction rate i.e. first order with respect to solid and gas reactant fits the data far better than other models such as shrinking core models, first order models, single grain models or crackling core model (Figure 6). However, all models including the selected one fail to predict the slowdown in the rate at conversions above 0.8 (Figure 7). It was also found that the observed slowdown cannot be attributed to the decrease in pellet effective diffusivity. The model incor-

porated the theoretical prediction for the decrease in diffusivity but could not match the experimental conversion curves at high conversion. On the other hand, it was found that theoretical predictions of the decrease in effective pellet diffusivity exceed considerably the actual experimentally determined reduction in effective diffusivity. The slowdown of reaction at high conversions can only be explained by changes in the micropore structure of the grains which we did not have the experimental capability to measure at present. The summary of experimental runs is given in Table III.

The apparent activation energy for the rate of reaction is obtained from Figure 8 as E_{app} = 5.5 kcal/mole. Clearly, the assumed rate form is affected by diffusion in the grains. The activation energy determined from the initial rates is E = 14.9 kcal/mol which should be close to the true kinetic activation energy. The points for all the runs lie on the straight line in Figure 8, indicating that the apparent kinetic constant is independent of pressure under which the pellet was made, as should be the case, and that it depends only on kinetics and diffusion in the grains. The temperature dependence of effective diffusivity can be expressed by a power function as shown in Figure 9 or by an Arrhenius form as shown in Figure 10. The values of effective diffusivities depend on the pressure at which the pellets were made. The slopes of the lines giving the temperature dependence increase with decrease in pellet manufacturing pressure. This is to be expected since at lower pellet manufacturing pressures the mean pore size is larger than at higher pressures. This means that at lower manufacturing pressures the relative contribution to overall diffusivity of molecular diffusivity with its $T^{3/2}$ temperature dependence as compared to Knudsen diffusivity with its $T^{1/2}$ dependence is more pronounced than at higher

manufacturing pressures. The experimentally determined temperature power coefficients vary from 1.38 to 1.06 and the corresponding "diffusion activation energies" from 2.05 to 1.46 kcal/mol for pellets manufactured from 4500 psia to 8000 psia. This agrees well with the dependence predicted from steady state measurements. Further details of data interpretation are given in the thesis by Lamba.

The research on modelling and development of new more efficient computational techniques was described previously and is summarized in the appended publications.

It was shown that a rather general model for gas-solid noncatalytic reactions which is described by two coupled partial differential equations can be reduced by an integral transformation to a set of initial value problems in space or in time. Since modern computers are so well suited for solution of initial value problems, the method provides significant advantages over Crank-Nicholson and other finite difference schemes.

In another development it was demonstrated that the change of coordinates permits the immobilization of the moving boundary between partly and fully reacted solid and allows efficient implementation of orthogonal collocation. The method again gives substantial savings in computational effort as compared to finite difference techniques. The method can readily be extended to systems with variable diffusivity as shown by Lamba in his thesis.

Analytical solutions are developed for a model where the reaction is Zeroth order with respect to the diffusing species which is a limiting case for

systems with strong adsorption. It was shown that the model predicts conversion-time relationships very similar to predictions of other more cumbersome models.

RESEARCH ACCOMPLISHMENTS

The following main accomplishments have been achieved by this research:

1. It was demonstrated experimentally that silicofluorides can be used successfully as fluorinating agents of halogenated hydrocarbons at temperatures as low as 300°C and that temperatures in excess of 600°C which previously were considered necessary can be avoided.

2. It was shown that for a reaction between barium fluoride and carbontetrachloride changes in structure of the solid are related to the change in solid molar density. This change in structure stops the reaction short of complete conversion in spite of the fact that the effective diffusivity through the pellet is not that much reduced. This seems to be due to the changes in micropore structure of the grains. Considerable additional work is necessary for proper and complete quantification of this phenomenon.

3. The kinetic and diffusions parameters and their temperature dependence for the above reaction were evaluated.

4. A number of new computational techniques for models of gas-solid reactions were introduced. These techniques reduce significantly the computational costs in comparison to currently available methods.

5. It was shown that a boundary value problem with moving boundary for a system of partial differential equations can be reduced to a set of initial value problems in time.

TABLE I

Apparent Density and Porosity Values

For The Pellets Used

Compound	Pressure At Which The Pellet Is Made (p.s.i.)					
	4500		6000		8000	
	Density gm/cm^3	Porosity	Density gm/cm^3	Porosity	Density gm/cm^3	Porosity
Barium Silico Fluoride	2.05	0.522	2.30	0.464	2.56	0.403
Barium Fluoride	2.62	0.464	2.74	0.440	2.90	0.407
Barium Chloride	2.01	0.482	2.21	0.430	2.30	0.406

TABLE II

Physical and Thermodynamic Properties of

the Solids and Reactions

Compound	Molecular Weight gm/gm mole	Density gm/cm^3	Molar Volume cm^3/gm mole	Solubility gm/100 ml	
				Cold Water	Hot Water
$BaCl_2$ α	208.25	3.856	54.007	37.5	59
$BaCl_2$ β	208.25	3.917	53.166	37.5	59
BaF_2	175.34	4.890	35.857	0.12	Sl.Sol.
$BaSiF_6$	279.42	4.290	65.132	0.026	0.09

Table III

Results for the Experimental Runs of Barium Fluoride with Carbon Tetrachloride

Run #	Pellet Produced at (p.s.i.)	Radius of the Pellet (cm)	Reaction Temperature °K(°C)	Kinetic Constant $cm^3/gm\ mole\ sec$	Effective Diffusivity cm^3/sec Experimental Run	Effective Diffusivity cm^3/sec Independent Experiment	Thiele Modulus
46	4500	0.4765	693(420)	35.65	0.0768	0.0314	1.25
41		0.4800	713(440)	40.00	0.0777	0.0326	1.33
39		0.4665	743(470)	45.83	0.0838	0.0343	1.33
37		0.4570	758(485)	49.57	0.0868	0.0352	1.33
19	6000	0.3175	658(385)	30.33	0.0671	0.0267	0.84
45		0.4665	698(425)	36.67	0.0726	0.0288	1.30
40		0.2200	713(440)	40.00	0.0744	0.0296	0.63
42		0.4805	713(440)	41.67	0.0725	0.0296	1.43
20	8000	0.4230	633(360)	24.76	0.0570	0.0182	1.13
44		0.4855	698(425)	37.50	0.0639	0.0206	1.51
43		0.4890	743(470)	50.00	0.0675	0.0223	1.71

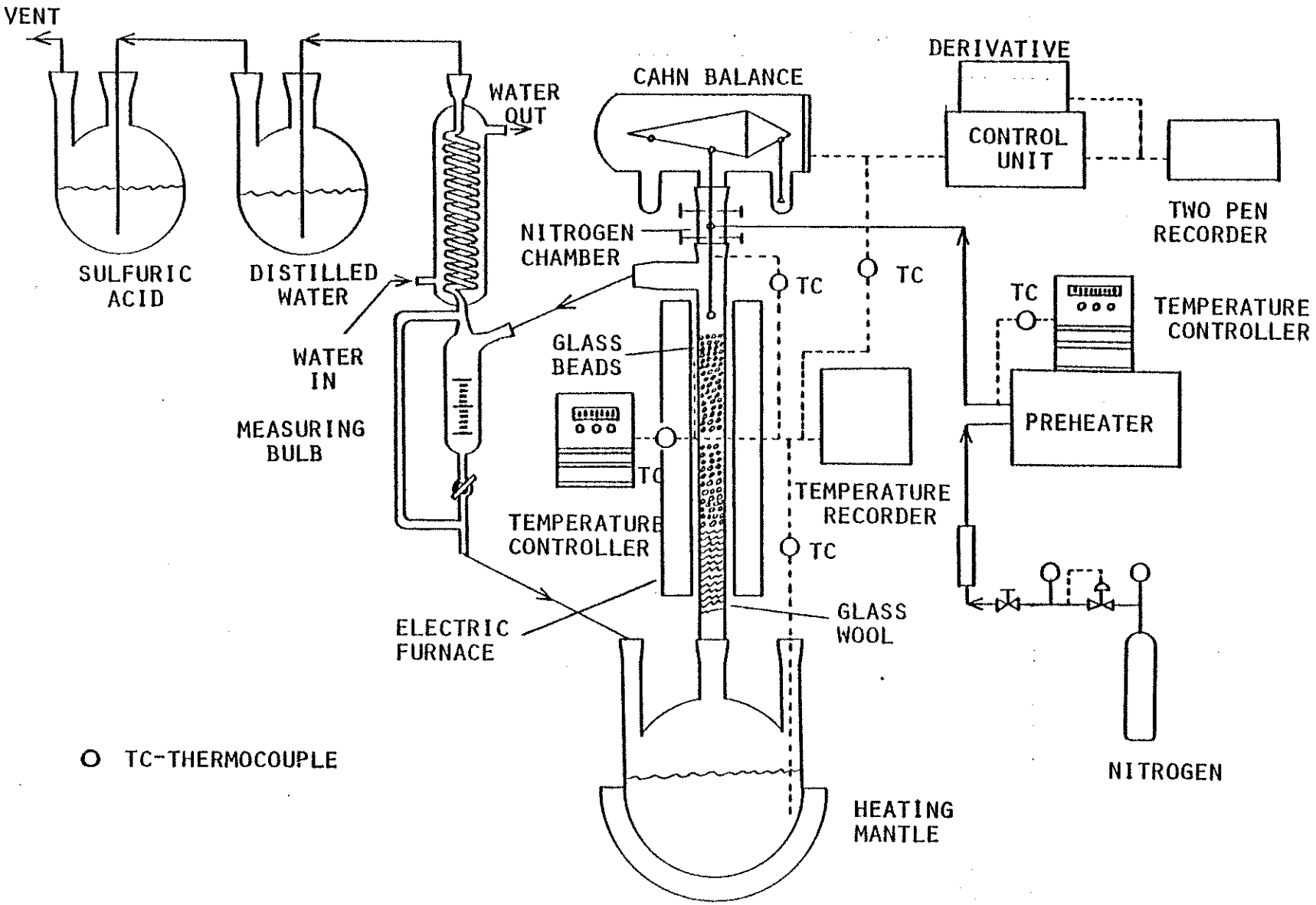

Figure 1. Experimental Setup

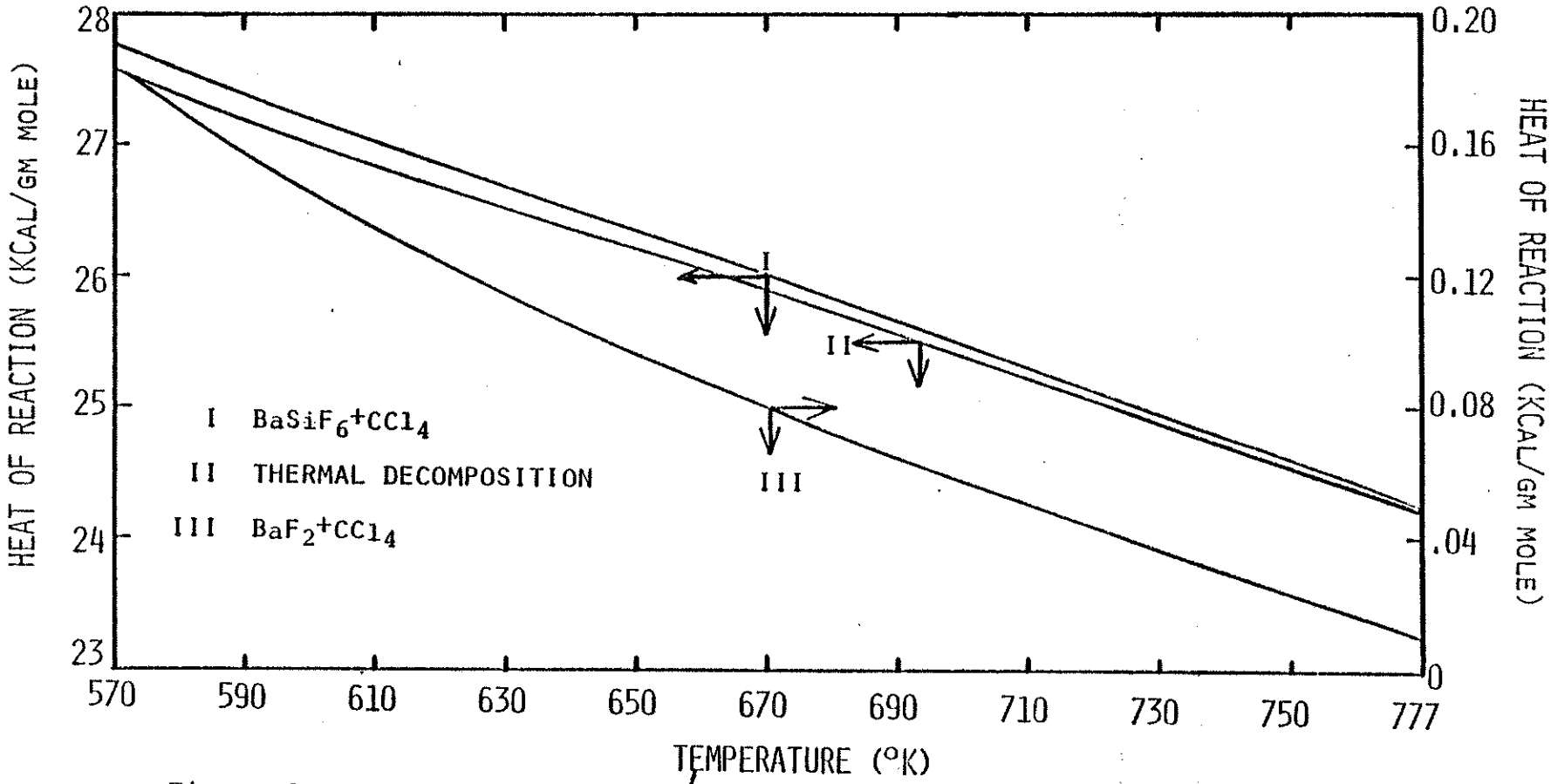

Figure 2. Heat of Reaction as a Function of Temperature for the Reactions Investigated

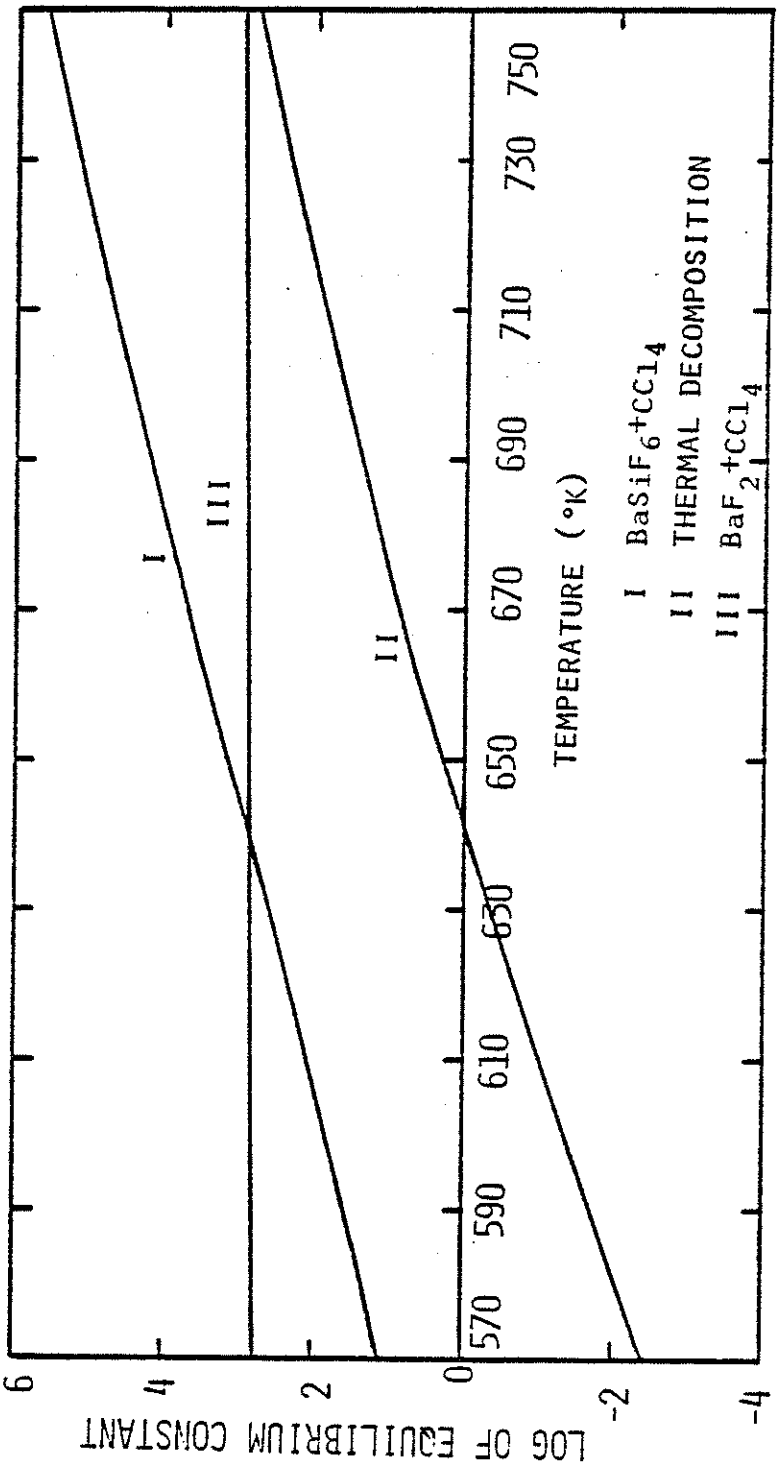

Figure 3. Effect of Temperature on the Equilibrium Constant of the Reactions Investigated

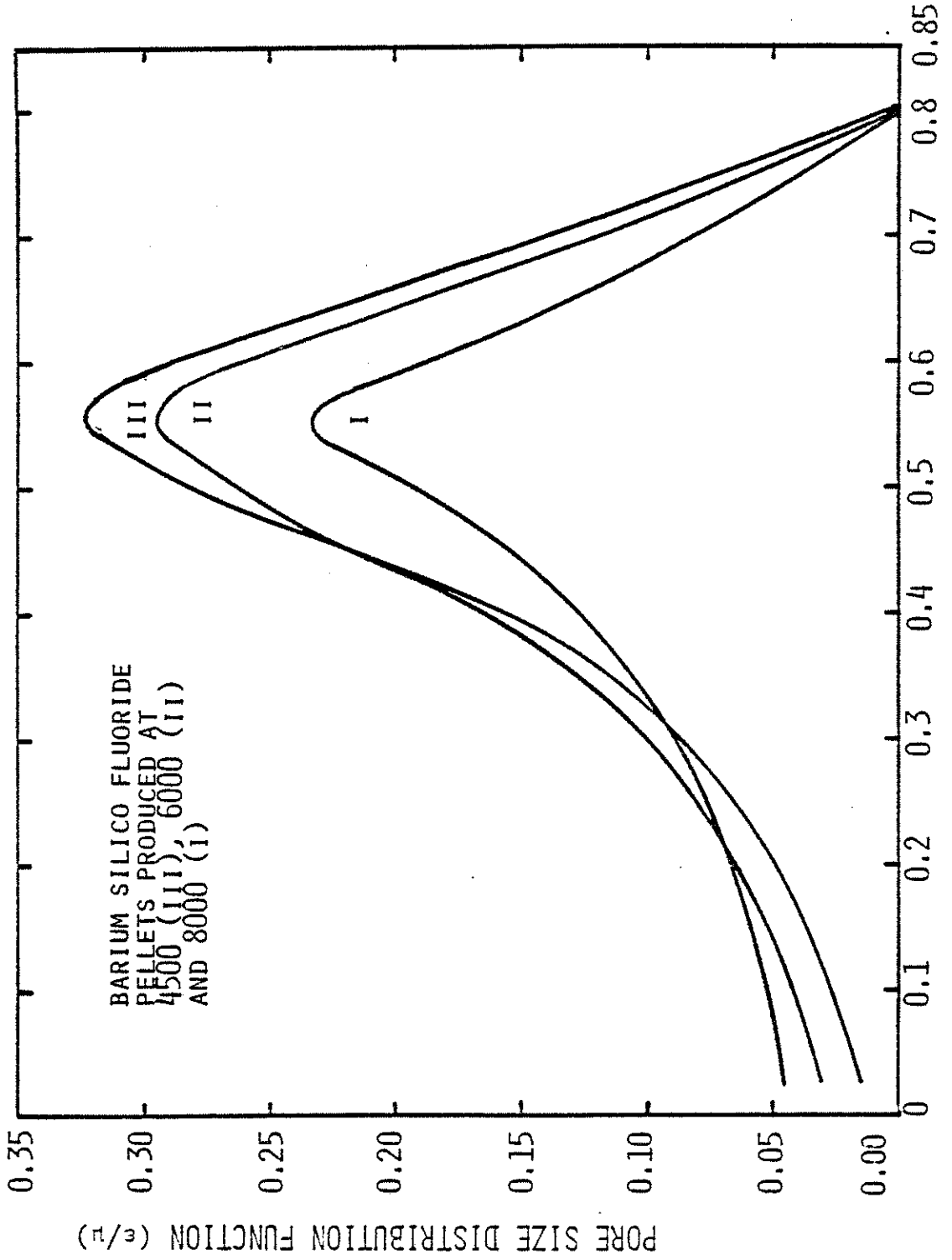

Figure 4. Pore Size Distribution of Unreacted Barium Silico Fluoride Pellets

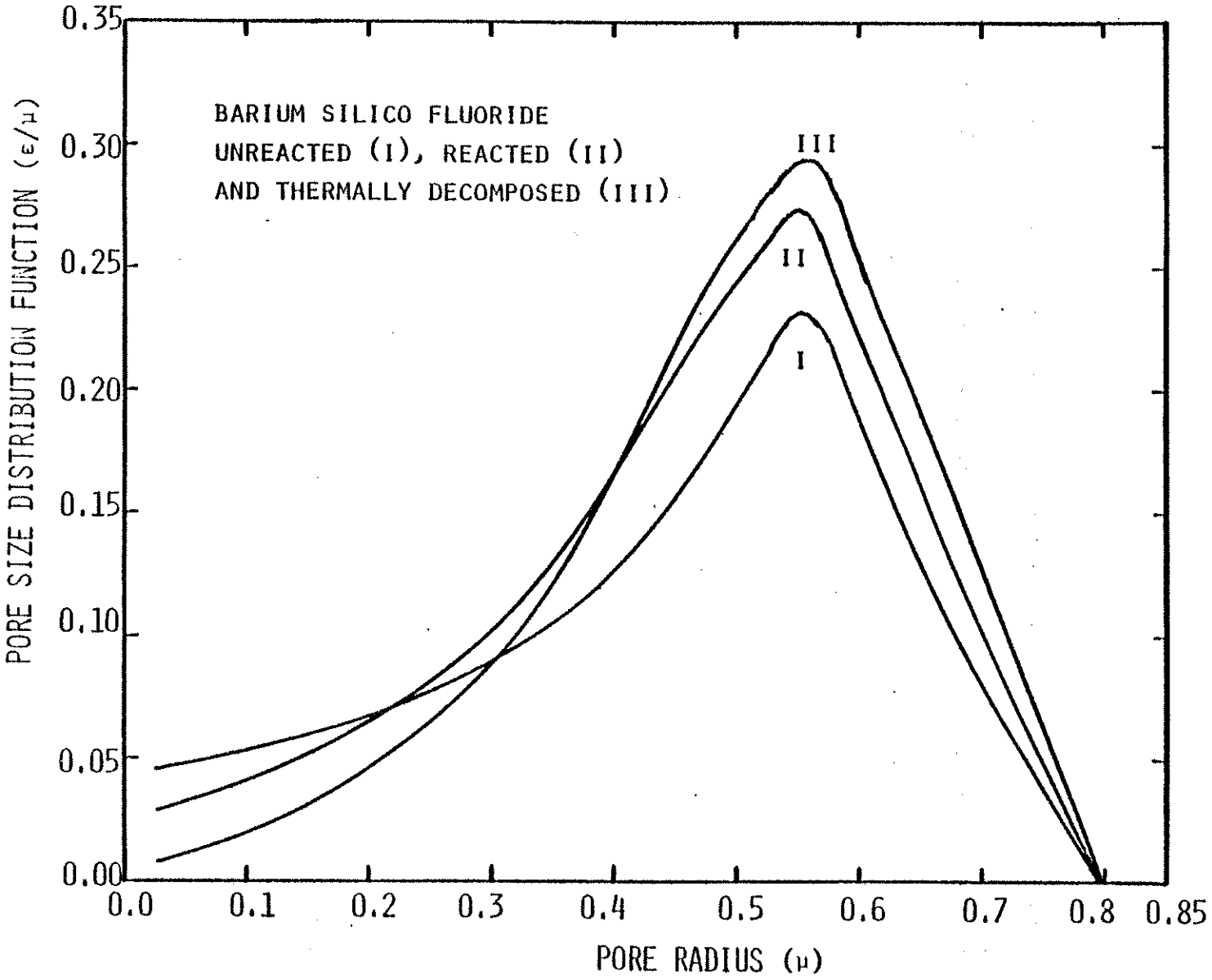

Figure 5. Pore Size Distribution of Unreacted and Reacted Barium Silico Fluoride Pellets Produced at 8000 p.s.i.

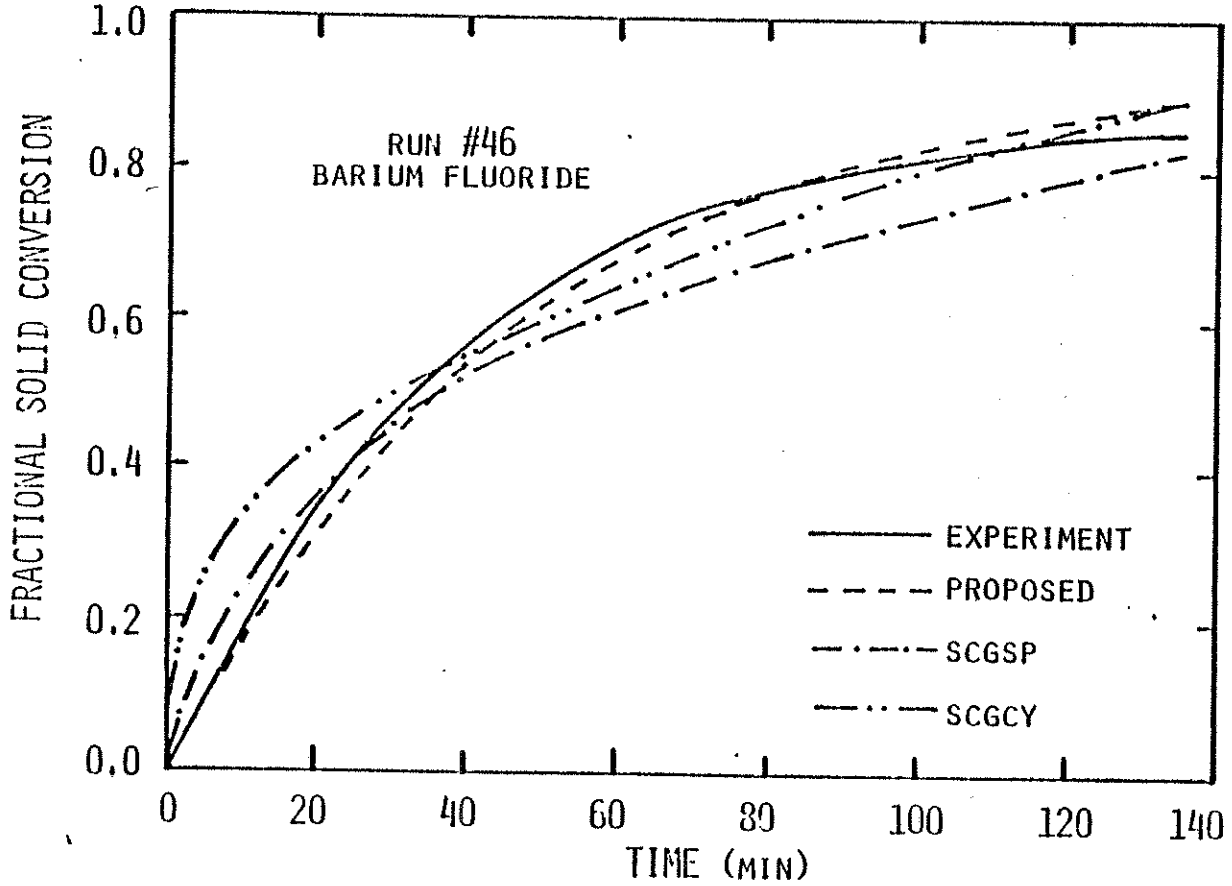

Figure 6. Comparison of Experimental and Predicted Solid Conversion as a Function of Time with Shrinking Core Models with Changing Grain Size

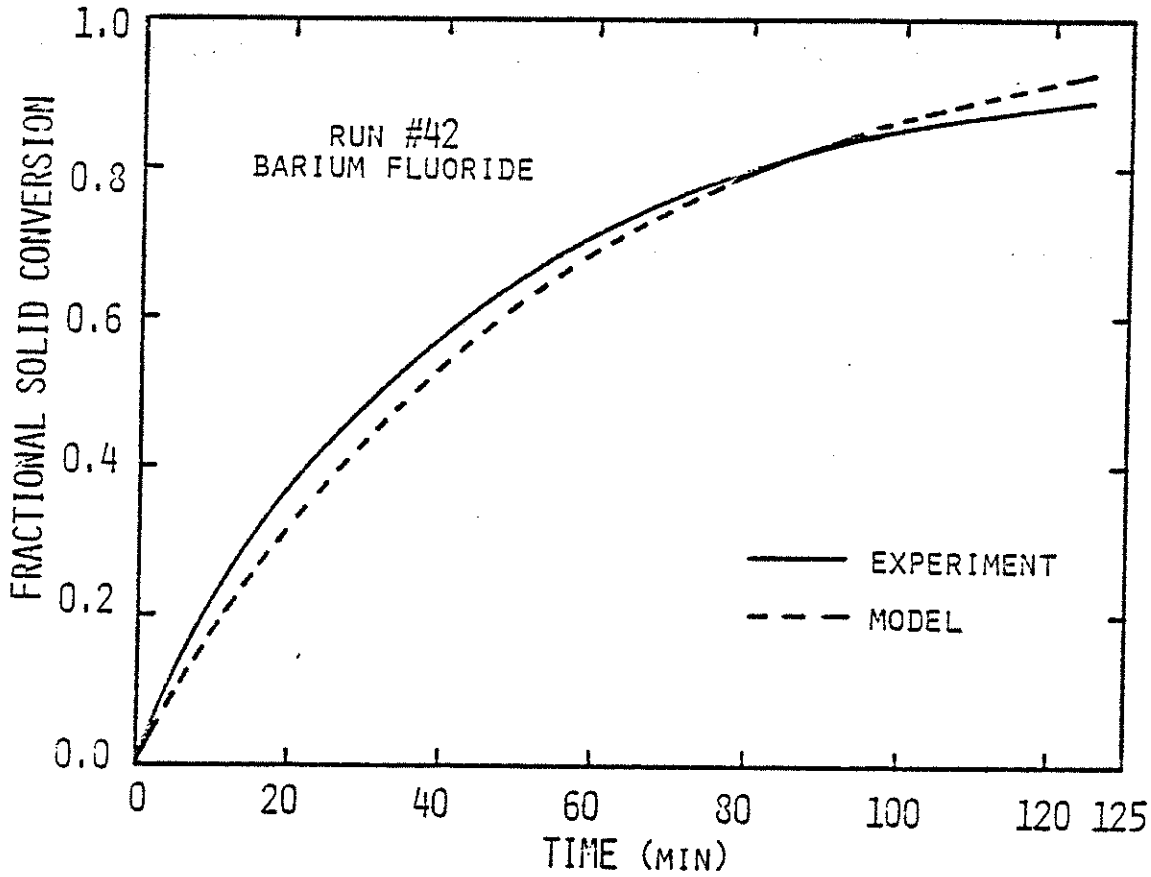

Figure 7. Match between the Experimental and the Predicted Solid Conversion as a Function of Time

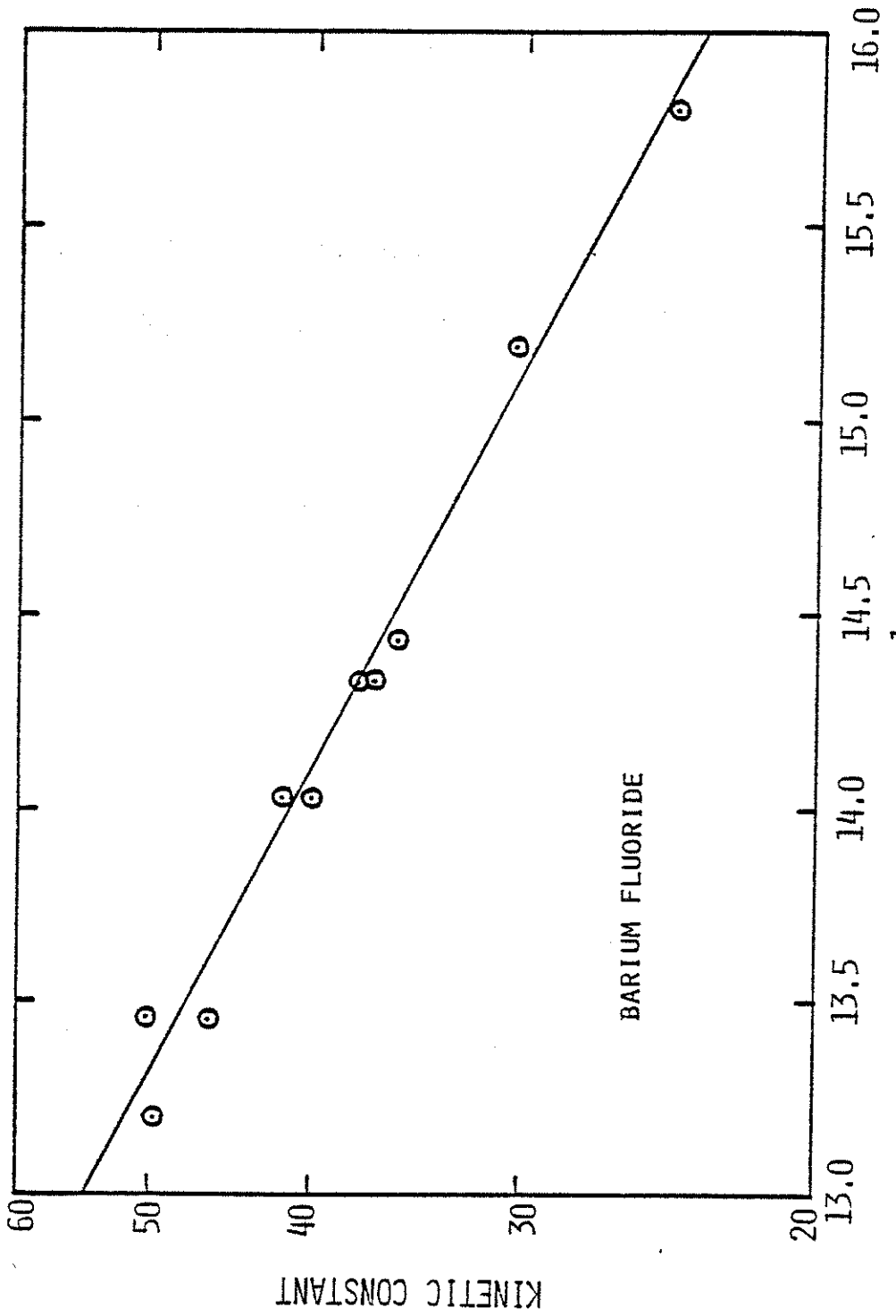

Figure 8. Arrhenius Plot for the Kinetic Constant Found from Two Parameter Estimation

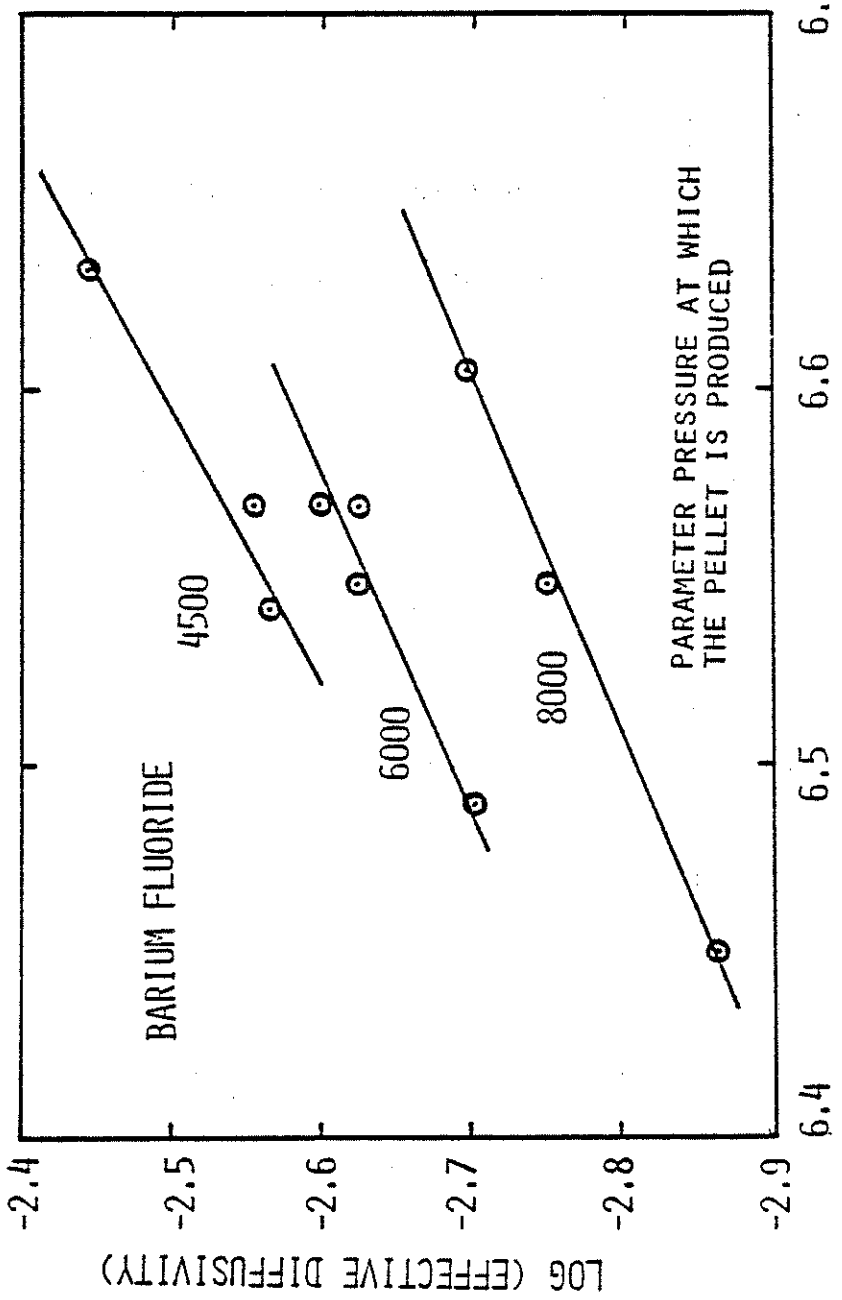

Figure 9. Power Law Dependence of Effective Diffusivity on Temperature

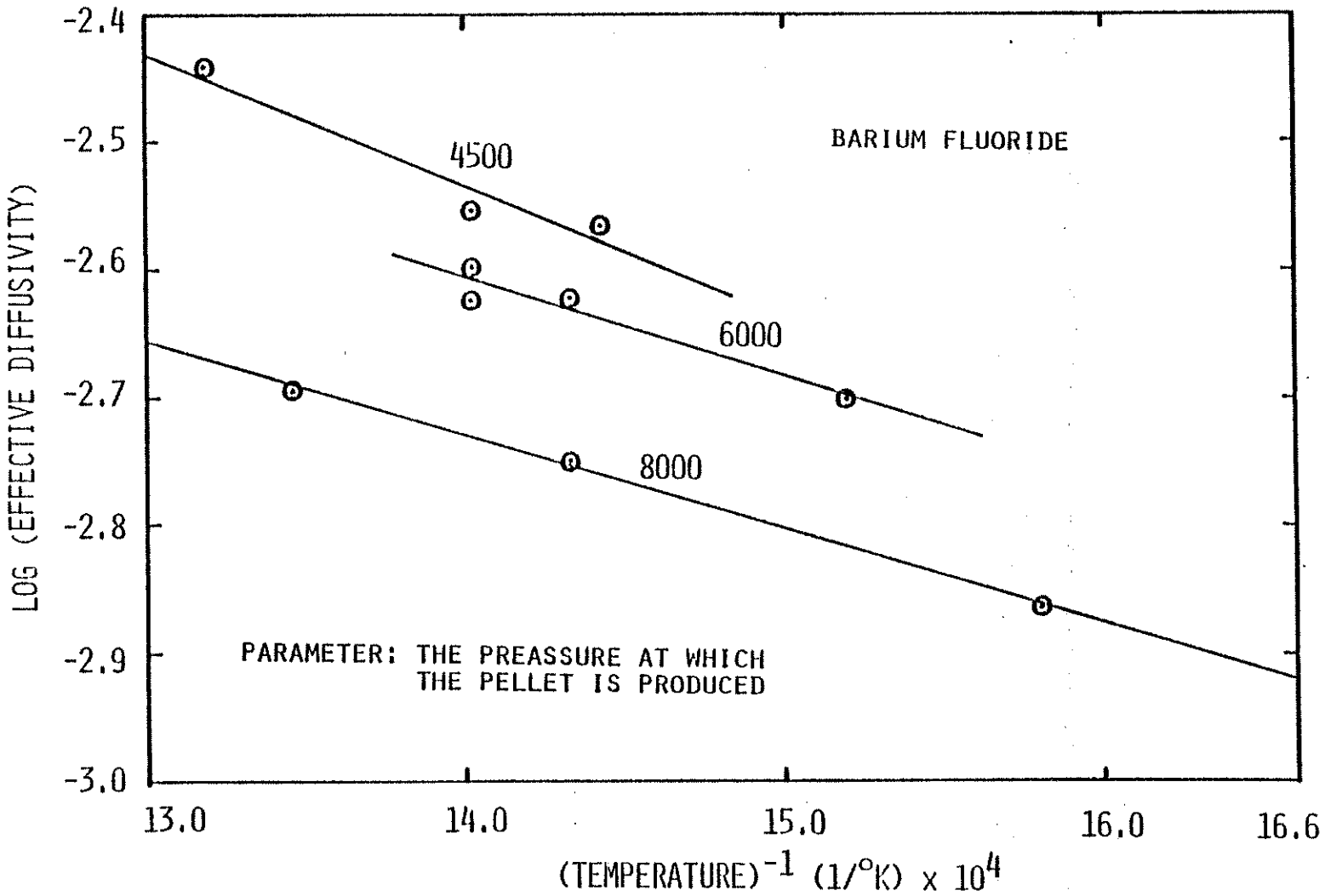

Figure 10. Arrhenius Plot for the Effective Diffusivity Found by Two Parameter Estimation

APPENDIX B

APPARATUS FOR TRACER

STUDIES IN TRICKLE-BED REACTORS

Figure 1: Revised Equipment for Tracer Reaction Studies

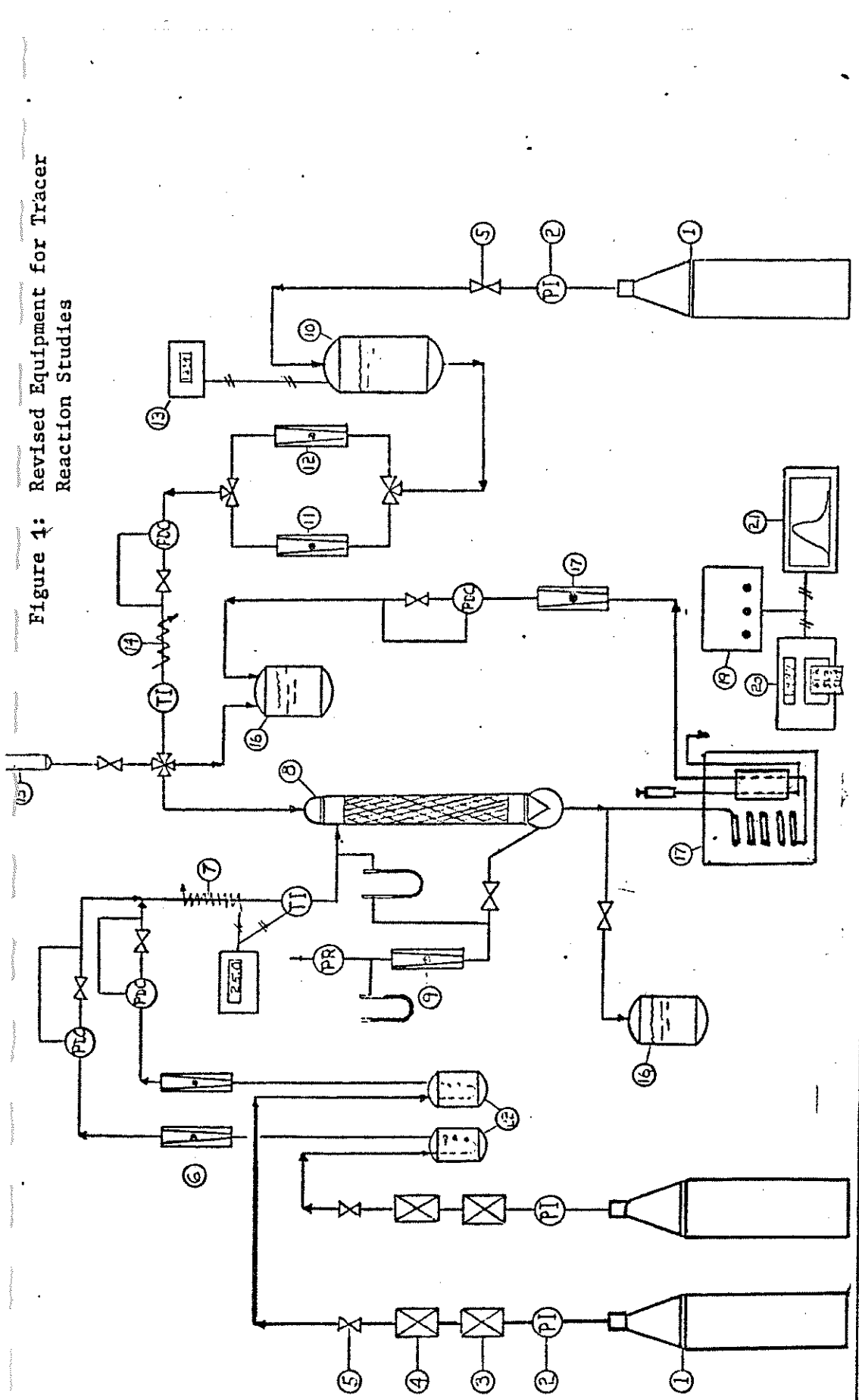

No.	Item	No.	Item	No.	Item
1	Gas Supply Cylinder	8	Trickle-Bed Column	15	Tracer Supply Tank
2	Pressure Indicator and Regulator	9	Outlet Gas Flowmeter	16	Waste Tank
3	Oxygen Trap	10	Liquid Supply Tank	17	Water Bath
4	Moisture Filter	11	Low Range Liquid Flowmeter	18	Optical Detector
5	Shut-Off Valve	12	High Range Liquid Flowmeter	19	Control Module
6	Inlet Gas Flowmeter	13	Bourdon Gauge	20	Voltmeter-Printer
7	Gas Heater	14	Liquid Feed Heater	21	Recorder
				22	Saturation Tanks

Figure 2: Revised Equipment for Tracer Reaction Studies

```
**********FLOW CHART TBR PROGRAM**********
*  THIS IS A DETAILED FLOW CHART FOR BOTH THE   *
*  PDP AND IBM VERSION OF THE TRICKLE BED       *
*  REACTOR DATA REDUCATION SYSTEM.              *
************************************************
```

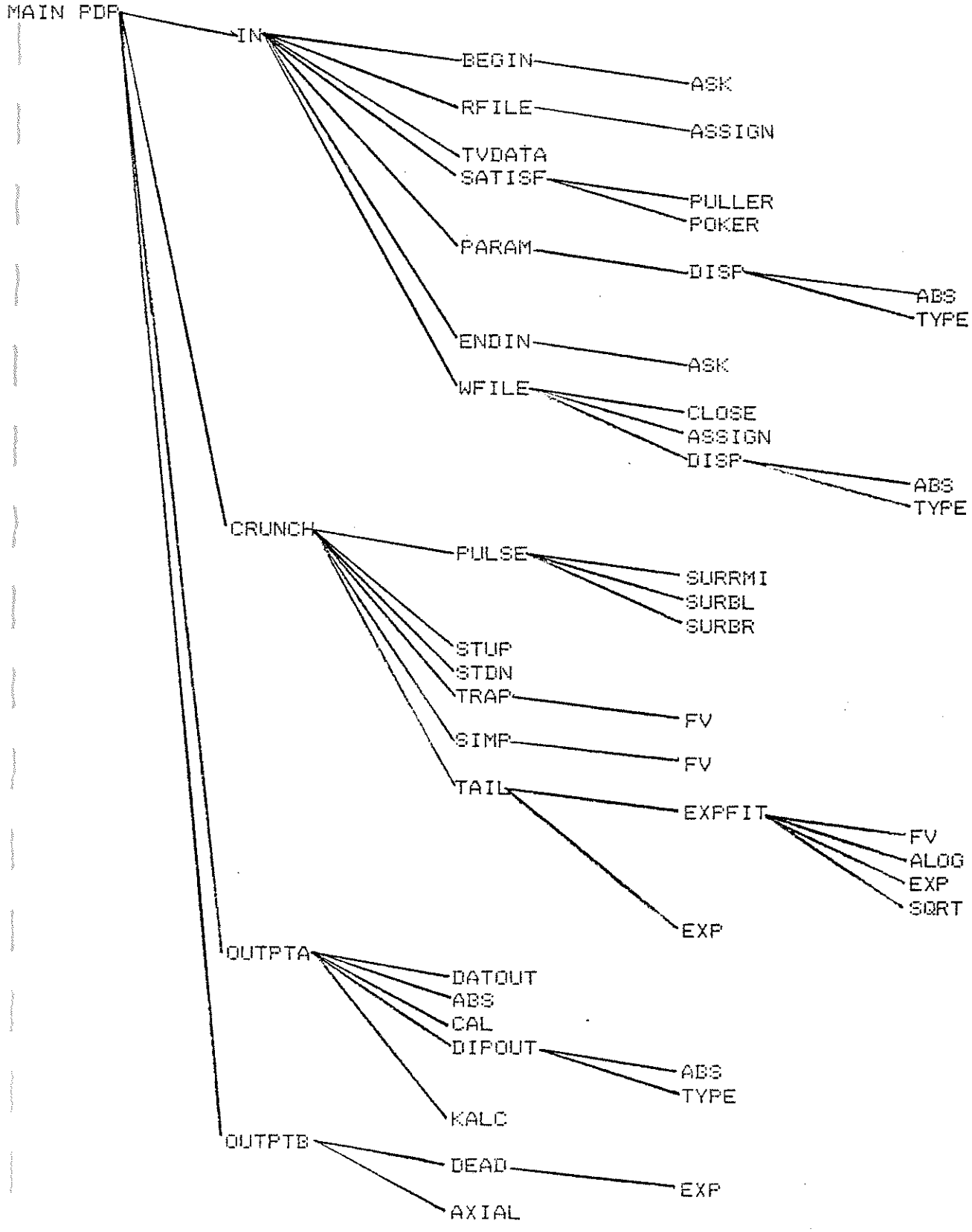

II. DESCRIPTION OF PROGRAM OPERATION

The TBR (TricKle Bed Reactor) program system is divided into three main functional sections as subroutines coordinated by a single main routine. The first section allows the user to input data from a CRT keyboard, create data files, and edit new data or data entered from a data file which is already on the system. This first section is coordinated by subroutine IN-

The second section is implemented through subroutine CRUNCH, and, as implied by the name, its function is the analysis of the time-voltage data. This analysis includes the calculation of the zeroth, first, ans second moments of the concentration-time curve.

The third section of the program system, which processes and formats the output of the data, parameters, moments, mean residance times, and variances, consist of two subroutines, OUTPTA and OUTPTB, which coordinate a set of subroutines which finish off the calculations and output the data, parameters, and calculated values in a form suitable for reports.

The following flow chart shows the relationships between the subroutines and functions which make up -his system under the three main catagories which have just been outlined. The following paragraphs contain detailed descriptions of each of the major subroutines along with a list of the variables which each subroutine outputs to the CRT or line printer. A chart showing the meaning of all of the important variables and their relation to the subroutines is given in the appendices.

2.1 IN

The purpose of subroutine IN is to coordinate all of the input subroutines. This routine, as can be seen in the flow chart is the focal point from which all of the other input routines are called. There are no variables output by this routine.

2.2 BEGIN

Subroutine BEGIN initializes the input section of the system. The routine then requires the user to input certain parameters concerning the data set. These parameters include the name of the data set, whether or not it is already on file, and, if the set is not already on file, the type of data, the number of data points, and whether the data is evenly spaced with respect to time. If the data is evenly spaced with respect to time, the routine also requires the input of the time interval between data points. There are no variables output by this routine.

2.3 RFILE

This routine is designed to read the information stored on a data file of the type created by the input section of the system. This information includes the data set name, the data set type, whether the data is evenly spaced with respect to time, and the time interval. The routine also reads the time and voltage vectors, the number of points, and the list of physical parameters entered in subroutine PARAM. This routine is highly specialized in that the data files are highly structured. This is because the data sets in the files are set up so that they are stored in readable form. Subroutine RFILE does not output any variables.

2.4 TVDATA

Subroutine TVDATA is the routine which reads the time-voltage data from the CRT keyboard if the data set is not being read from a data file. In doing this, the routine produces output on the CRT screen which aids in entering the data, such as numbering the points as they are entered. This routine also uses the parameters entered in BEGIN to generate the time vector so that only the voltage vector need be input for evenly spaced data. The generated values appear on the CRT screen next to the index of the data point. The value of the voltage vector at that position must be entered beside the generated time value. This routine does not output any variables.

2.5 ASK

ASK is a PDP 11 Macro routine which reads a null terminated (carriage return terminated) character string from the CRT keyboard and returns the string in a left justified array. This array must be initialized to blanks before calling ASK since the routine does not change any more of the positions of the array than are necessary to fit in the character string. The routine also returns a count of the characters in the input string. No variables are output from this routine.

2.6 PULLER

This subroutine is designed to remove a value from a specified position in a vector and readjust the positions of the other values in the vector to fill in the empty position. This routine is general in that it will accept a vector of any length, as specified in the parameter list. There are no output variables in this subroutine.

2.7 POKER

Subroutine POKER is designed to place a value in a vector, first moving all of the other values so as to vacate the specified position. This routine increases the vector length by one position. Like subroutine PULLER, subroutine POKER is a general routine in that it can be used on any length vector. The routine has no output variables.

2.8 PARAM

PARAM is a routine which is designed for entering and editing experimintal parameters. The routine starts by asking for each of the parameters if the data is not being read from a file. If the data is being read from a file, this section is replaced by a call to subroutine DISP, which displays the current parameter values. The routine also allows for the editing of the parameters, one at a time, as referenced by the number under which they are displayed. Each pass through the routine has one of three functions. The first of these functions is the entering of all of the parameters. This is only done for a new data set. The second function is that of an editor. One parameter may be edited per pass. The last function is merely a call to subroutine DISP, which , as mentioned earlier, displays the current parameter values.

2.9 DISP

This routine outputs the parameters entered in subroutine PARAM. This output is structured in such a way that each parameter is labeled and numbered , The numbering system is primarily for the referencing of a parameter in the editing procedure in subroutine PARAM. The output of this routine may be routed to either the CRT screen, as in subroutine

PARAM, or to a sequential access, formated data file, as in subroutine WFILE. The output variables are given below.

PARA(11) - Array containing the eleven experimental parameters

2.10 ENDIN

Subroutine ENDIN determines if you wish to create a data file. In doing this, you may use a completely new name, or you may update an existing file by writing over it. The PDP 11 filing system will not permit the existance of more than one file with the same name, therefore, the last file written under a given name is the only one which will be present on the disk. Because of this, subroutine ENDIN contains an option allowing the user to change the name under which a file is written. There are no output variables in this routine.

2.11 WFILE

This routine writes a sequential access, formated data file containing all of the input data. First, it writes a header containing the data set name, data type, whether the data is evenly spaced, and the time interval for evenly spaced data. It then writes the experimental parameters using subroutine DISP. Finally, it writes the number of data points and the time and voltage vectors. The output variables, which contain all of the input variables, are given below.

T(500) - Time data vector

V(500) - Voltage data vector

PARA(11) - Experimental parameter vector

NPT - Number of data points

ITYPE - Data set type (pulse, step up, or step down)

NAME - Array containing the data set name

TANS - Yes or No depending on whether the data is evenly spaced

DT - Time interval for evenly spaced data

2.12 SATISF

Subroutine SATISF provides for the editing of the time-voltage data. This is done in one of three ways. The first is deleting a point by removing it from both time and voltage vectors and updating the variable containing the number of points. The second is the analogous insertion of a point. The third editing feature allows for the insertion or deletion of a single value from one of the vectors, moving all of the other values up or down with respect to the other vector. This routine also displays the time and voltage data. The output variables are given below.

T(500) - Time data vector

V(500) - Voltage data vector

2.13 CRUNCH

Subroutine CRUNCH is the major routine tying together all of the calculational routines of the system. It calls routines for surveying pulse, step up, or step down tracer curves, and evaluates the moments of the curve using an exponential fit to extend the curve out to infinity. The following are the output variables.

A - Multiplier from the exponential fit

B - Exponential constant

R - Residual from the exponential fit

TM(3) - Array containing the contributions of the curve tail to the three moments of the curve.

M2(3) - Array containing the main contribution to the three moments

M(3) - Array containing the total moments of the concentration-

time curve.

2.14 PULSE

This routine analyses the data from the pulse tracer experiments. It calls a set of subroutines which survey the voltage-time curve for the critical values. The routine then calculates the base line drift correction and asks if it is to be used, after outputing the parameters for the correction. The routine then calculates the concentration vector. The following are the output variables.

BS - Base line correction slope

BY - Base line correction Y-intercept

2.15 SURMI

Subroutine SURMI is the part of the set of survey subroutines which finds the maximum point on the concentration-time curve and the inflection point on the left side of the surve. This routine may be used for both pulse and step up residence distribution time experimental data. This routine has no output variables.

2.16 SURBL

This is the part of the set of survey subroutines which finds the first point ont the left side of the curve greater than five percent of the maximum value and the point where the response begins. This routine may be used for both pulse and step up tracer studies. The routine has no output variables.

2.17 SURDR

This is the last of the set of survey routines. Its function is to

find the first point on the right side of the curve which has a value greater than five percent of the maximum value, the point at which the response ends, and the average of all of the values avter the end of the response. This routine may be used for pulse tracer and step down tracer studies. This routine has no output variables.

2.18 TRAP

The purpose of subroutine TRAP is to integrate a curve between two specified points. It accomplishes this by applying the trapazoidal rule to two vectors containing the points on the curve. The routine is used in the system for irregularly spaced (with respect to time) data points. This routine has no output variables.

2.19 SIMP

Subroutine SIMP integrates a curve with evenly spaced data points between two specified points. It accomplishes this using a Simpsin's Rule numerical integration. This method is more accurate than the integration using the trapazoidal rule, and is therefore used by the system to integrate all curves containing evenly spaced data. This routine only needs one input vector and a time interval. The routine has no output variables.

2.20 FV

FV is a function which evaluates the functional values needed in subroutines TRAP and SIMP from the concentration vector and time vector. It serves to evaluate functional values for any of the three moments, depending on an input parameter. The function has no output variables.

2.21 TAIL

Subroutine TAIL calls subroutine EXPFIT to fit an exponential curve to the last part of the concentration-time curve between two specified points. It also evaluates the contributions to each of the three moments from the extrapolation of this fitted curve to infinity. The routine has no output variables.

2.22 EXPFIT

Subroutine EXPFIT evaluates the constants in a curve fit of the data in two input vectors between two specified positions. The curve fit to the data is of the form $Y = A\ e^{BX}$ where A and B are the curve fit constants. This routine has no output variables.

2.23 OUTPTA

This routine is the first segment of the main part of the last section of the system. Its purpose is to start the job of putting the experimental data, experimental and calculated parameters, and resulting values of model parameters into readable form for inclusion in a report. First, the routine prints a header containing all of the information in the data file header. It then outputs the voltage, time, and concentration vectors using subroutine DATOUT, paging at appropriate intervals. An abreviated header is printed on each page following the first. Next, the routine calculates the flow rates from the rotameter settings using subroutine CAL, prints the experimental parameters using subroutine DIPOUT, and calculates and prints the calculated parameters using subroutine CALC. The output variables for this routine are as follows.

NAME(7) - Integer array containing the data set name

IPAGE - Output page number

2.24 OUTPTB

Subroutine OUTPTB is an extension of subroutine OUTPTA. It writes out the dead volume corrections to the mean residence time and variance from subroutine DEAD, the first three moments of the concentration-time curve, the uncorrected and corrected mean residence time and variance of the curve in both seconds and minutes, the dimensionless variance of the curve, and the bed and particle axial dispersion numbers calculated by two methods in subroutine AXIAL. The output variables are as follows.

DMRT	- Dead volume mean residence time (seconds)
DMRTM	- Dead volume meam residence time (minutes)
DVAR	- Dead volume variance (sq seconds)
DVARM	- Dead volume variance (sq minutes)
M(3)	- Array containing the three total moments of the curve
RMRT	- Uncorrected mean residence time (seconds)
RMRTM	- Uncorrected mean residence time (minutes)
RVAR	- Uncorrected variance (sq seconds)
RVARM	- Uncorrected variance (sq minutes)
CMRT	- Corrected mean residence time (seconds)
CMRTM	- Corrected mean residence time (minutes)
CVAR	- Corrected variance (sq seconds)
CVARM	- Corrected variance (sq minutes)
DIMVAR	- Dimensionless variance
BED1	- Bed dispersion number (method 1)
BED2	- Bed dispersion number (method 2)
PART1	- Particle dispersion number (method 1)
PART2	- Particle dispersion number (method 2)

2.25 DATOUT

This subroutine prints, in tabular form, the time voltage and concentration vectors between two specified positions. It is necessary to specify the positions in order that the output may be paged properly in subroutine OUTPTA. The output variables are as follows.

T(500) - Time data vector

V(500) - Voltage data vector

C(500) - Concentration data vector

2.26 CAL

Subroutine CAL evaluates a set of flow rates from an input of rotameter settings. This is done by evaluating the fifth order polynomial obtained from a least squares analysis of the calibration curves of each of the three flow meters. The number of the flow meter and the scale which is being read is specified in the input to the subroutine. There are no output variables in this routine.

2.27 DIPOUT

Subroutine DIPOUT serves exactly the same function for the output section of the system as subroutine DISP serves for the input section. The only difference between the two routines is that subroutine DIPOUT contains an extra set of variables which prints the corresponding flow rate beside each rotameter setting. The flow rates are the same as those calculated in subroutine CAL. The output variables are as follows.

PARA(11) - Experimental parameters (array)

RF(3) - Array containing the flow rates corresponding to the three rotameter settings

2.28 KALC

Subroutine KALC calculates and prints a set of numbers which describe the experimental system for a particular run. These numbers include the liquid hourly space velocity, the mass superficial velocities, the superficial velocities, and the liquid and gas side Reynold's numbers. The output variables for this routine are as follow.

CALA(7) - Array containing the calculated parameters

2.29 DEAD

Subroutine DEAD calculates the dead volume correction for the mean residence time and variance by evaluating the fifth order polynomial obtained by a linear least squares analysis of the curve obtained from the processed data from a set of runs of tracer studies on the dead volume. This routine has no output variables.

2.30 AXIAL

Subroutine AXIAL calculates two values of the bed axial dispersion number using two different nonlinear equations. The numbers are calculated by evaluating the fifth order polynomial from the linear least squares analysis of the curves generated by the two equations.

The first method uses the following equation.

$$\sigma^2 = 2(D_a/ U_L L) - 2(D_a/ U_L L)^2 \ (1 - \exp[-U_L L/ D_a])$$

The second equation uses this equation.

$$\sigma^2 = 2(D_a/ U_L L) - (D_a/U_L L)^2 \ [\exp(-2U_L L/D_a) + 4\exp(-U_L L/D_a) + 4(U_L L/D_a)\exp(-U_L L/D_a) - 5]$$

The routine has no output variables.

DATA SET NAME --- NA15

KIND OF DATA --- IRREGULARLY TIMED SAMPLING

MODE OF OPERATION --- PULSE TRACER

EXPERIMENTAL DATA

INDEX	TIME (SEC)	VOLTAGE (MV)	CONCENTRATION
1	0. 00000	0. 00000	0. 000000
2	30. 40000	0. 00000	0. 000000
3	32. 40000	4. 20000	4. 20000
4	34. 60000	9. 80000	9. 80000
5	36. 00000	26. 00000	26. 0000
6	38. 40000	46. 50000	46. 5000
7	40. 80000	61. 00000	61. 0000
8	42. 00000	65. 50000	65. 5000
9	43. 20000	68. 00000	68. 0000
10	44. 40000	68. 60000	68. 6000
11	45. 60000	67. 30000	67. 3000
12	46. 80000	65. 00000	65. 0000
13	50. 40000	54. 70000	54. 7000
14	52. 80000	47. 50000	47. 5000
15	56. 40000	37. 30000	37. 3000
16	58. 80000	32. 00000	32. 0000
17	62. 40000	25. 00000	25. 0000
18	66. 00000	20. 00000	20. 0000
19	68. 40000	17. 20000	17. 2000
20	70. 80000	15. 00000	15. 0000
21	74. 40000	11. 60000	11. 6000
22	76. 80000	10. 00000	10. 0000
23	80. 40000	8. 20000	8. 20000
24	86. 40000	5. 00000	5. 00000
25	92. 40000	4. 00000	4. 00000
26	98. 40000	3. 00000	3. 00000
27	104. 40000	2. 00000	2. 00000
28	110. 40000	1. 20000	1. 20000
29	116. 40000	0. 90000	0. 899999
30	130. 80000	0. 00000	0. 000000

OPERATION PARAMETERS

1)	CALIBRATION FACTOR (GM/CC/MV)	=	1.000		
	ROTAMETERS		SETTING	FLOW RATE (CC/MIN)	
2)	-- REFRACTOMETER	=	14.000	31.806	GLASS
3)	-- LIQUID INLET	=	15.000	33.441	GLASS
4)	-- GAS INLET	=	9.000	62.097	GLASS
	DENSITIES (GM/CC)				
5)	-- LIQUID	=	0.6571		
6)	-- GAS	=	0.1647E-03		
	VISCOSITIES (CP)				
7)	-- LIQUID	=	0.3157		
8)	-- GAS	=	0.1800E-01		
9)	REACTOR DIAMETER (CM)	=	1.350		
10)	PACKING HEIGHT (CM)	=	30.00		
11)	PARTICLE DIAMETER (MM)	=	0.7180		

CALCULATED PARAMETERS

A)	LIQUID HOURLY SPACE VELOCITY (1/HR)	=	46.725
	MASS SUPERFICIAL VELOCITY (KG/SQ M/SEC)		
B)	-- LIQUID	=	3.575
C)	-- GAS	=	0.6856E-04
	SUPERFICIAL VELOCITY (CM/SEC)		
D)	-- LIQUID	=	0.5440
E)	-- GAS	=	0.4163E-01
	REYNOLDS NUMBERS		
F)	-- LIQUID	=	8.131
G)	-- GAS	=	0.003

		SEC	MIN
DEAD VOLUME - MEAN RESIDENCE TIME	=	5.6294	0.0938
		SQ SEC	SQ MIN
- VARIANCE	=	2.5250	0.0007

RESULTS

ZEROTH MOMENT	=		1731.78589
FIRST MOMENT	=		94299.39844
SECOND MOMENT	=		5582495.00000
		SEC	MIN
MEAN RESIDENCE TIME	=	54.4521	0.9075
CORRECTED MEAN RESIDENCE TIME	=	48.8227	0.8137
		SQ SEC	SQ MIN
VARIANCE	=	258.5159	0.0718
CORRECTED VARIANCE	=	255.9909	0.0711
DIMENSONLESS VARIANCE	=		0.1074
		METHOD 1	METHOD 2
AXIAL DISPERSION NUMBER (BED)	=	0.0552	0.0644
AXIAL DISPERSION NUMBER (PARTICLE)	=	0.0013	0.0015

APPENDIX C

PREDICTION OF GAS HOLDUP AND LIQUID RECIRCULATION IN A GAS-LIFT RECYCLE REACTOR

ABSTRACT

Experimental study on gas holdup and liquid recirculation rates in gas-lift loop reactors was conducted with air-water system in a 1.25 inch (3.2 cm) inside diameter and 4 ft. (122 cm) tall gas-lift model equipment. Results of gas holdup were correlated with a total superficial velocity of the two-phase gas liquid flow. The correlations of holdup were incorporated into a momentum balance equation from which liquid recirculation rates at given gas injection rates can be calculated for a fixed gas-lift loop configuration. The calculated recirculation rates were in close agreement with the experimental measurements.

INTRODUCTION

The use of gas-lift loop reactors shows promise of increasing applications in chemical industry, particularly for liquid phase oxidation and hydrogenation processes involving a high concentration of suspended catalyst particles and highly exothermic reactions. The attractive features of gas-lift reactors are mainly due to the liquid recirculation which is induced by injecting gas reactants into a gas-lift upleg and which provides excellent liquid phase mixing, tends to uniformly suspend the solid particles and brings the reactor to an essentially isothermal operation. The gas-lift reactor eliminates the need for a mechanical agitator, as required in the conventional stirred tank reactor, and can provide higher heat transfer surface per unit liquid volume and higher mass and heat transfer coefficients than those normally obtained in bubble columns.

Other advantages with the gas-lift loop reactor are: feasibility of high pressure operation; continuous catalyst withdrawal for regeneration; relatively easy scale up when compared to bubble columns or trickle bed reactors from the standpoint of imperfect mixing and catalyst wetting.

Disadvantages with the gas-lift loop reactor include, however, the difficulty of handling suspended solids in the system and removal of solid particles from the liquid product and possibilities of poor yields of intermediates due to high liquid backmixing.

Due to the lack of complete knowledge in design and operation, especially in the area of predicting the liquid recirculation and handling the solid suspension, among other things, the gas-lift reactor has not been very popular in chemical industry. The recent progress in the knowledge of two-phase pipe flows has, needless to say, increased the understanding of gas-lift operation and provided valuable information for the design and scale up.

It is necessary and important for a process design engineer to be able to estimate the liquid recirculation rate of a given gas-lift loop at a specified gas injection rate during the course of reactor design and scale up. Liquid velocity in the two phase reactor upleg is a design and scale up parameter that affects the gas void fraction (i.e. gas holdup); thus, residence times of gas and liquid, mass and heat transfer coefficients, and the mixing characteristic of liquid reactants and products.

Gas-lift loop reactors employ the same basic concept of pumping liquid by compressed air in an air-lift pump, the theory and performance of which have been discussed in several published papers (1,2,3). This published information, however, is not directly applicable to the gas-lift reactor design due to the differences in geometrical setups and operating conditions. An air-lift pump is normally designed to operate in slug flow in order to obtain its best efficiency. It consists of no recycle downleg. Therefore, the resistance to the liquid pumping rate (i.e. pressure drop) is mainly in the two-phase lift tube. On the other hand, the gas-lift loop reactor consists of a gas-lift upleg and a liquid recycle downleg with a gas-liquid separator setting on the top of the

two legs. The pressure drop in the downleg provides additional resistance to the liquid recirculation. The desirable flow regime for the gas-lift reactor operation is often in bubble or froth flow, rather than slug flow, in order to maximize the gas-liquid interfacial area as frequently required to improve mass transfer rate in a gas-liquid reaction process. Large slugs bridging the diameter of the tube of a commercial size reactor may never exist, and the froth regime requires high gas injection rates; thus, a high consumption of gas or an increased compression requirement for recycling the unreacted gas as compared to the bubble flow operation. The bubble flow, including certain degrees of bubble coalescence, is of interest to the design and operation of a gas-lift loop reactor, yet this is the regime that requires further investigations in both hydrodynamics and mass transfer.

The present objective of this research is to undertake the study of the inter-relationship between the gas holdup and liquid recirculation in a gas-lift apparatus and obtain, eventually, design and scale up information for the commercial gas-lift reactors. At present, experimental results included in this paper were obtained from a 1.25 inch (3.2 cm) diameter gas-lift apparatus. Further investigations on larger units are in progress.

THEORY

The recirculation of liquid in a gas-lift loop reactor is caused by a density difference between a two-phase upleg and a practically gas-free liquid recycle downleg. The rate of liquid recirculation depends primarily on the gas injection rate, diameters and heights of the loop tubes, and to a substantial degree, on the configuration of the reactor loop.

As shown in Figure 1, the driving force for the liquid to flow from the downleg into the upleg is provided by the hydrostatic head difference between the two legs. Under steady state operation, the hydrostatic head difference must equal the pressure drop in both legs. The pressure drop includes frictional drops at tube walls, a liquid acceleration loss across the gas injection point and pressure losses due to the entrance to the downleg and to the discharge from the upleg.

The bubble flow pattern encountered in the gas-lift reactor allows the use of pseudo homogeneous friction factor concept for the pressure drop calculations (4).

Assuming H_D and H_U denote heights of the downleg and the upleg respectively, an overall momentum balance equation for the gas-lift loop can be readily written:

$$\underbrace{[\varepsilon_G \rho_G + (1- \varepsilon_G) \rho_L]_D H_D}_{\text{Hydrostatic head of downleg}} - \underbrace{[\varepsilon_G \rho_G + (1 - \varepsilon_G) \rho_L]_U H_U}_{\text{Hydrostatic head of upleg}} =$$

$$\Big[\underbrace{\frac{4f_L L}{D_t}\left(\frac{\rho_M V_M^2}{2g_c}\right)}_{\text{Frictional Drop of upleg}} + \underbrace{K_1 \frac{\rho_M V_M^2}{2g_c}}_{\text{Exit loss of upleg}} + \underbrace{\frac{\rho_L V_L}{g_c}\left(\frac{V_L}{1-\varepsilon_G} - V_L\right)}_{\text{Acceleration loss across the gas injection}}\Big]_U + \underbrace{\Big[\frac{4f_L L}{D_t}\left(\frac{\rho_M V_M^2}{2g_c}\right)}_{\text{Frictional drop of downleg}}$$

$$+ \underbrace{K_2 \frac{\rho_M V_M^2}{2g_c}}_{\text{Downleg entry loss}} + \underbrace{K_3 \frac{\rho_M V_M^2}{2g_c}\Big]_D}_{\text{Other losses due to values, bends, etc.}} \qquad (1)$$

where $V_M = V_G + V_L$ (2)

$$\rho_M = \rho_L (1 - \varepsilon_G) + \rho_G \varepsilon_G \simeq \rho_L (1 - \varepsilon_G) \qquad (3)$$

and K's are numbers of velocity head losses. In practice, $K_1 = 1.0$ for the exit loss of the upleg; $K_2 = 0.5$ for the entry loss of the downleg and K_3, the sum of losses due to value and fitting in the downleg, may be obtained elsewhere (5). V_M, total velocity of the gas-liquid mixture, is the sum of superficial gas and liquid velocities (V_G and V_L) based on the cross sectional area of the pipe.

f_L, Fanning's friction factor, is determined from conventional Reynolds number - friction factor plot using a Reynolds number defined as follows:

$$Re_{,M} = \frac{D_t V_M \rho_L}{\mu_L} \qquad (4)$$

The gas holdup, ε_G, is the volume fraction of the pipe occupied by gas. The holdup in the downleg is normally unknown. It depends on the amount of gas bubbles entrained from the separator by the downflowing recycle liquid. This gas entrainment, in turn, is dependent upon the adequacy of the separator performance. In most cases, the entrained gas could be minimized by maintaining a sufficient liquid level in the separator, in addition to proper sizing of the separator and its internal baffles for vortex breaking.

If the entrained gas and, thus, the gas holdup in the downleg can be neglected, then after proper rearrangement, the momentum balance equation, Eq. (1) may be simplified as:

$$\underbrace{H_D - (1 - \varepsilon_G) H_U}_{\substack{\text{Hydrostatic head difference} \\ \text{between downleg and upleg,} \\ \text{in feet of liquid.}}} = \underbrace{\left(1 + \frac{4f_L L_U}{D_{tU}}\right) \frac{V_M^2}{2g_c} (1 - \varepsilon_G)}_{\substack{\text{Total pressure drop} \\ \text{of upleg}}} + \underbrace{\frac{V_L^2}{g_c} \left(\frac{\varepsilon_G}{1-\varepsilon_G}\right)}_{\substack{\text{Acceleration} \\ \text{loss across gas} \\ \text{injection}}} + \underbrace{\left(K + \frac{4f_L' L_D}{D_{tD}}\right) \frac{V_L^2}{2g_c} \left(\frac{D_{tU}}{D_{tD}}\right)^4}_{\substack{\text{Total pressure drop} \\ \text{of downleg}}} \qquad (5)$$

The second term of RHS, the pressure loss due to the liquid velocity increase passing the gas injection point, is normally negligible. Within our experiments, the term accounts for less than 1% of the total pressure drop of the system.

Here V_L in Eq. (5) is based on the upleg, so the liquid velocity in the downleg, having a diameter of D_{tD}, is equal to V_L in the upleg multiplied by

by a correction factor for the diameters as shown in the last term of the equation.

The equation can be used to calculate the liquid recirculation rate, in terms of V_L in a fixed gas-lift equipment of predetermined diameters and heights for a given gas injection rate (i.e. V_G in the upleg). Since the gas holdup, ϵ_G, appears in the equation as a function of V_L as well as V_G, the solution for V_L is not explicit. The calculation requiring additional relationships between the gas holdup and velocities of gas and liquid (V_L and V_G) may be performed by trial and error. The gas holdup correlations for two-phase flow system are discussed below.

Based on the review of Hill (6), there are two semi-theoretical methods of correlating data on gas holdup as a function of V_G and V_L. The first method is to correlate the slip velocity between the gas bubbles and the liquid as a function of rising velocity of single bubble and of hindering effect of neighbouring bubbles, either in terms of gas holdup (6), or superficial gas velocity (7). This method may be applicable to the regime of uniform bubbling.

The second method considers bubbles rising into the liquid above them. The apparent mean bubble velocity, V_G/ϵ_G, is correlated as a function of total velocity as:

$$\frac{V_G}{\epsilon_G} = C_o\ (V_G + V_L) + U_B \qquad (6)$$

When applying (6) to fully developed slug flow, $U_B = 0.35\ (g\ D_t)^{\frac{1}{2}}$ is the free rise velocity of a slug in stagnant water and $C_o = 1.20$, allows for a non-

uniform liquid velocity profile, based on Nicklin et. al. (8).

Equation (6) has also been used successfully for coalescing bubble flow in pipes either too wide or too short to permit the formation of slugs bridging the column diameter (6, 9, 14).

Other correlations include the well-known Martinelli method (10) and those by Hughmark (11) among many others (12, 13). It was found in our experiments that Eq. (6) could be satisfactorily used.

EXPERIMENTAL

For the investigation of gas holdup and liquid recirculation of gas-lift reactors, a plexiglass apparatus was constructed. The apparatus, shown in Figure 2, consists of a 1.25" i.d. by 4 feet long vertical upleg, a .75" i.d. downleg and a cylindrical gas-liquid separator having 8 inches in diameter and 10 inches in height. Along the length of the upleg, six manometers spaced equally at 8-inch intervals are provided for monitoring the void fraction in the upleg.

The gas-liquid separator is connected with a level control cylinder of 4" diameter by 8" long. The cylinder can be moved manually in vertical direction to control the liquid level in the separator.

At present, the equipment has been tested with air-water system. The compressed air was introduced through a rotameter and dispersed into the bottom of the upleg by a porous glass dispersion tube (Model 124-529, having a 12 mm disc, made by Curtin Scientific).

Experiments covered a range of operating conditions with gas superficial velocities up to approximately .8 ft/sec and liquid superficial velocities up to 1.2 ft/sec.

To avoid additional restriction to the liquid recirculation, no flow restriction valve or flow measuring device was provided in the reactor loop.

The liquid recirculation rates at a fixed gas rate were altered by changing the liquid height in the downleg. The recirculation flow rates were measured by an external measuring tank during experimental runs with one-through operation without liquid recycle, as shown by Figure 2.

A vertical partition was installed in the separator to isolate the discharged liquid of the upleg from the downleg compartment in which the liquid level was maintained by continuous makeup of liquid. Any excess of the makeup liquid was drained through the overflow line of the level control tank so that a desired liquid level was maintained.

The above one-through continuous flow operation should simulate the gas-lift recycle operation without the partition in the separator. The amount of the discharged liquid collected in the measuring tank within a fixed time period allows a direct and accurate measurement of the liquid recirculation rate.

The gas holdup in the upleg was calculated from the manometer reading with a correction for the pressure drop in the upleg. The pressure drop was found significant only at high velocities tested.

If the height of the two-phase upleg is H_U, the clear water height in the manometer is h and the pressure drop through the upleg is h', then the gas holdup can be calculated by:

$$\varepsilon_G = \frac{H_U - (h - h')}{H_U} \tag{7}$$

and

$$h' = \left(1 + \frac{4f_L H_U}{D_t}\right)\frac{V_M^2}{2g_c} \qquad (8)$$

Without the pressure drop correction for the manometer reading, the error on the gas holdup could amount to over 10% for the high velocities encountered in our experiments.

RESULTS

1. Flow Regime and Gas Holdup

Flow patterns encountered in our experiments in the 1.25" diameter lift tube are in uniform bubble to coalescing bubble flow regime. Large bubble slug was experienced in the upper velocity region. An experimental run was normally terminated before the slug flow was reached, because unstable slugging prevent accurate reading on the monometer, and a further increase of gas injection beyond this point would not noticeably increase the liquid recirculation rate.

Measured holdup data were used to calculate apparent mean bubble velocities (i.e. V_G/ε_G). These values were then plotted against total mixture velocities (i.e. $V_M = V_G + V_L$), as shown in Figure 3. Initially, it was found from the plot that data were scattered without any trend, especially at low velocities. But then, a closer review of the data revealed that two distinct trends of correlations could represent the data considered. As indicated in Figure 3, lines having a deeper slope roughly represent data with a gas holdup greater than 0.2, and those having a smaller slope belong to data with 0.2 or less gas holdup. This result seems to be logical, since in the high gas holdup region, gas bubbles coalesce more significantly and, thus, the mean bubble velocity of the coalescing bubbles increases more rapidly when compared to the situation with low gas holdup.

The two correlations that best fit our data of the 1.25 inch gas-lift tube were obtained by a linear regression method as below:

For $\varepsilon_G \leq 0.2$

$$\frac{V_G}{\varepsilon_G} = .81 + .92\ (V_G + V_L) \tag{9}$$

For $\varepsilon_G > 0.2$

$$\frac{V_G}{\varepsilon_G} = .36 + 1.4\ (V_G + V_L) \tag{10}$$

Eq. (9) and (10) are shown in Figure 4 and 5 respectively for the comparison with experimental data and the available slug flow correlations of Nicklin et. al. (2) and Ellis (9).

The choice between (9) and (10) depends on the gas holdup. The gas holdup, as discussed perviously, is dependent upon, not only the gas velocity, but also the liquid velocity, as can be seen from the plot in Figure 6. Since the gas holdup is a dependent variable, it is, therefore, required to define the transition between the two correlations in terms of V_G and V_L. To do this, a horizontal line representing the transition holdup of 0.2 was drawn across data curves in Figure 6. The points of the line were then plotted in Figure 7 as the transitional gas velocity, V_{GT}, as a function of liquid velocity V_L. A straight line roughly represents these transition points at $\varepsilon_G = 0.2$ was resulted:

$$V_{GT} = .146 + 2.63\ V_L \tag{11}$$

At a given V_L, any superficial gas velocities that are greater than V_{GT} calculated from (11) (i.e. $V_G > V_{GT}$), will result in $\varepsilon_G > 0.2$; therefore,

Eq. (10) should be used. On the contrary, if $V_G \leq V_{GT}$ at a given V_L, then $\varepsilon_G \leq 0.2$ and Eq. (9) should be used.

The correlation of Ellis and that of Nicklin et. al. seem to be in close agreement with our data for $\varepsilon_G > 0.2$, as shown in Figure 5. Nevertheless, these correlations do not agree so well with the data for $\varepsilon_G \leq 0.2$, as shown in Figure 4. It should be noted that the correlations presented here by Eqs. (9), (10) and (11) are based solely on our air-water data obtained from the 1.25 inch diameter gas-lift apparatus. These correlations should be expanded to cover the effect of diameters before applying them to a commercial size gas-lift reactor design.

2. Liquid Recirculation

Typical results of experimental runs are shown in Figure 8, where measured liquid recirculation rates in terms of superficial liquid velocities and their corresponding gas holdups were plotted against superficial gas velocities. As indicated by the data, the liquid rate increases rapidly at first with increasing gas rate but very slowly at high gas rates. This is expected, because as the gas velocity increases, the holdup value approaches an asymtote as a result of increasing bubble coalescence, and, at the same time, the pressure drop of the system increases and put, eventually, a limit to the liquid recirculation. The gas-lift apparatus shows an optimum efficiency of liquid recirculation capacity at superficial gas velocities between .1 and .2 ft/sec, where one cubic foot of gas input produces approximately three cubic feet of liquid recirculation

(i.e. $V_L/V_G \simeq 3$). The capacity reduces to $V_L/V_G \simeq 1.5$ when V_G reaches .8 ft/sec. Although not shown by the data, the liquid recirculation rate should eventually reach a maximum if the gas rate increases further.

The measured liquid recirculation rates at various gas rates and liquid heights of the downleg were compared with calculated values based on the momentum equation, Eq. (5). The comparison is quite satisfactory, as shown in Figure 9. The K value, which accounts for the pressure drop of the downleg other than wall friction, was found to be about 3.0 based on the experiment with the setup shown in Figure 2. This experimental K value agrees closely with published data (5) shown below:

1 - Entry loss at downleg	= 0.5
1 - 90° standard elbow	= 0.75
1 - Tee	= 1.5
Total K	= 2.75

Some experiments were run with modified separator internals, which increase the froth at the outlet of the upleg by an additional 2 inches. During these experimental runs, the liquid outlet from the upleg must flow over a rectangular weir before entering the liquid flow measuring tank. This resulted in additional pressure drop to the system as reflected by the increase of K value from 3.0 to 4.0.

The 4 curves shown in Figure 9 were calculated from Eqs. (5), (9) and (10). The curves show a sudden break in slope at superficial gas velocity equals to

about 0.3 ft/sec. This break reflects the transition for the holdup correlations, (9) and (10), based on the criterion given by (11). The sudden slow-down of the V_L increase after the transition point agrees quite well with the data.

The trial and error calculation for the liquid recirculation rates was performed successfully with a pocket size programmable calculator (TI59 by Texas Instruments).

CONCLUSION

Based on the result of the 1.25" gas-lift apparatus, the following conclusions are obtained:

1. A flow transition was defined by Equation (11). Below the transition velocity (or $\varepsilon_G \leq 0.2$) bubbles rise uniformly without significant coalescence. The gas holdup in this flow regime obeys Eq. (9). Above the transition point (or $\varepsilon_G > 0.2$), the bubble coalescence becomes very significant. A different correlation, such as Eq. (10), can be used.

2. The momentum equation, Eq. (5), is recommended for predicting a liquid recirculation rate in a predetermined gas-lift configuration for a given gas injection rate, V_G. The equation should be applicable to any commercial size gas-lift loop reactors, provided a proper gas holdup correlation for large diameter tubes is used. The correlations of gas holdup, as resulted from this study, has not included the effect of tube diameters.

3. Operation of a gas-lift loop reactor in the slugging flow regime should be avoided, because of high gas consumption, low efficiency of liquid recirculation and poor gas-liquid interfacial area for mass transfer. Future study on large diameter gas-lift apparatus should be concentrated in bubbly flow to coalescing flow regime.

4. The liquid recirculation rate of a gas-lift loop reactor depends on the liquid height in the separater, the gas injection rate (thus, the holdup in the upleg) and the equipment configuration. The optimum efficiency of liquid recir-

culation, expressed as V_L/V_G, lies in the bubbly flow regime before a significant bubble coalescence takes place (i.e. $\varepsilon_G \simeq 0.2$), as found in our 1.25" apparatus.

NOTATION

D_{tU} = diameter of upleg, ft.

D_{tD} = diameter of downleg, ft.

f_L = Fanning's friction factor

g_c = standard acceleration of gravity, 32.174 ft/sec^2

H_D = liquid height of downleg, ft.

H_U = liquid height of upleg, ft.

h = height of liquid in a manometer, ft.

h' = pressure drop in upleg, defined by (8), ft.

K = number of velocity head loss

L = length of tube, ft.

$Re_{,M}$ = Reynolds number, $\frac{D_t V_M \rho_L}{\mu_L}$

U_B = a constant or free rise velocity of a slug in stagnant water, ft/sec.

V_G = superficial gas velocity, ft/sec.

V_L = superficial liquid velocity, ft/sec.

V_M = total superficial velocity, $(V_G + V_L)$, ft/sec.

Greek Letters

ε_G = gas holdup defined as fractional volume of gas in tube.

μ_L = liquid viscosity, lbs/ft, sec.

ρ_G = gas density, lbs/ft^3

ρ_L = liquid density, lbs/ft^3

ρ_M = average density of gas-liquid mixture, lbs/ft^3

Subscripts

D = downleg

G = gas-phase

L = liquid-phase

M = mixture

GT = transitional gas velocity

t = tube

U = upleg

REFERENCES

1. Richardson, J. F. and Higson, D. J., "A Study of the Energy Losses Associated with the Operation of an Air-Lift Pump," Tran. Instn. Chem. Engrs., 40, 169, 1962.

2. Nicklin, D. J., "The Air-Lift Pump: Theory and Optimization," Tran. Instn. Chem. Engrs., 41, 29, 1963.

3. Stenning, A. H., and Martin, C. B., "An Analytical and Experimental Study of Air-Lift Pump Performance," Trans. of ASME, J. of Eng. for Power, 106, April, 1968.

4. Govier, G. W. and Aziz, K., "The Flow of Complex Mixtures in Pipes," Van Nostrand Reinhold Comp, P. 387, 1972.

5. Perry, R. H., Chilton, C. H. and Kirkpatrick, S. D., "Chemical Engineers' Handbook," McGraw-Hill Comp. 4th ed., P. 5-33, 1969.

6. Hill, J. H., "The Operation of a Bubble Column at High Throughputs, I. Gas Holdup Measurements," The Chem. Eng. J., 12, 89, 1976.

7. Towell, G. D., Strand, C. P. and Ackerman, G. H., "Mixing and Mass Transfer in Large Diameter Bubble Columns," A.I.Ch.E. - I. Chem. Eng. Symposium Series No. 10, 97, 1965.

8. Nicklin, D. J., Wilkes, J. O. and Davidson, J. F., Trans. Inst. Chem. Engrs., 40, 61, 1962.

9. Ellis, J. E., and Jones, E. L., "Vertical Gas-Liquid Flow Problems," Proceedings, Vol. 2, Symposium on Two Phase Flow, Uni. of Exeter, Devon, England, 1965.

10. Lockhart, R. W. and Martinelli, R. C., Chem. Eng. Prog., 45, 39, 1949.

11. Hughmark, G. A., "Holdup in Gas-Liquid Flow," Chem. Eng. Prog., 58, 62, 1962.

12. Griffith, P., "The Prediction of Low-Quality Boiling Voids," J. of Heat Transfer, Trans. ASME, Series C, 83, 307, 1961.

13. Bankoff, S. G., J. of Heat Transfer, Trans. ASME, Series C, 82, 265, 1960.

14. Zuber, N. and Findlay, J. D., J. Heat Transfer, Series C, 87, 453, 1965.

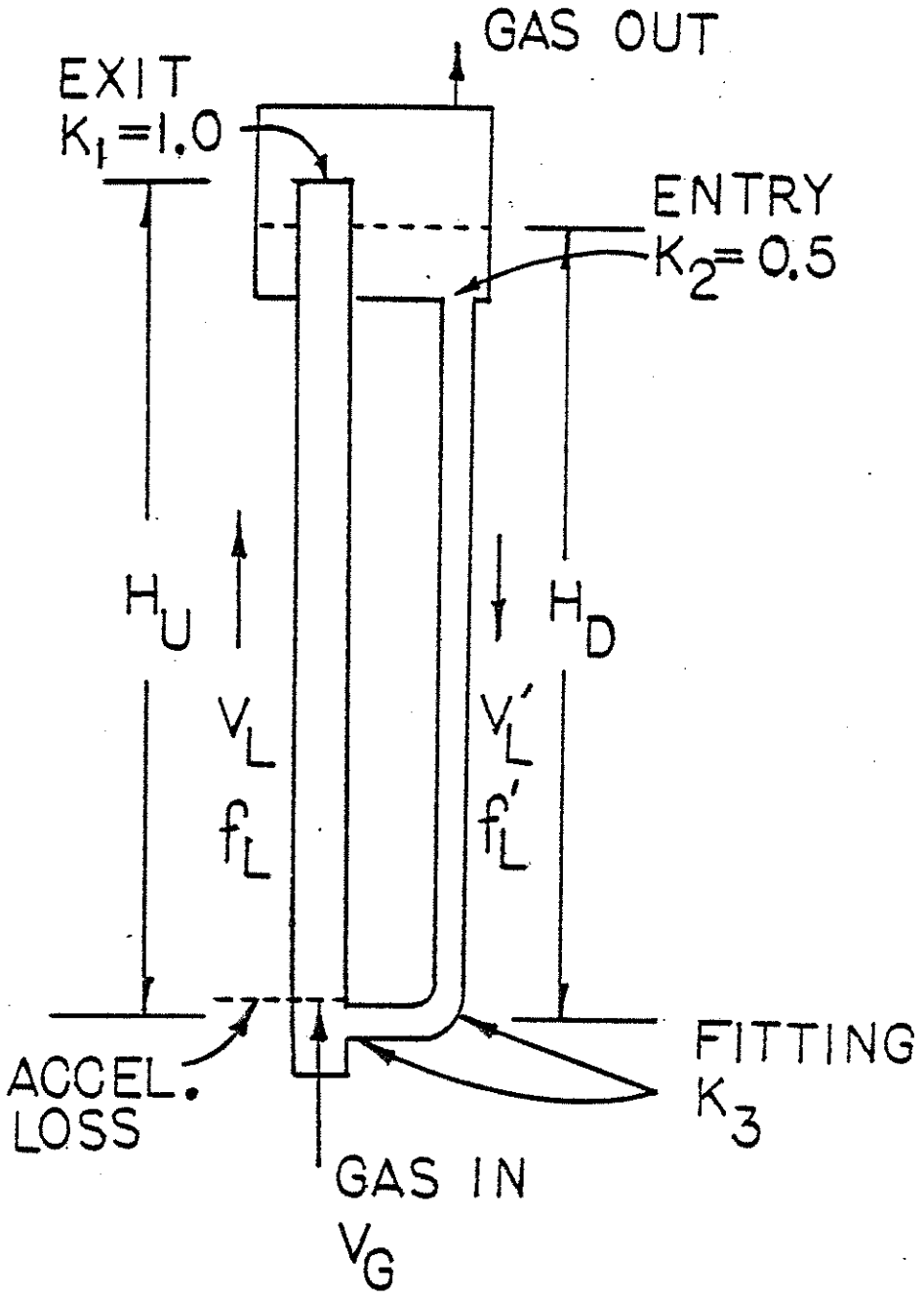

FIG 1 MOMENTUM BALANCE

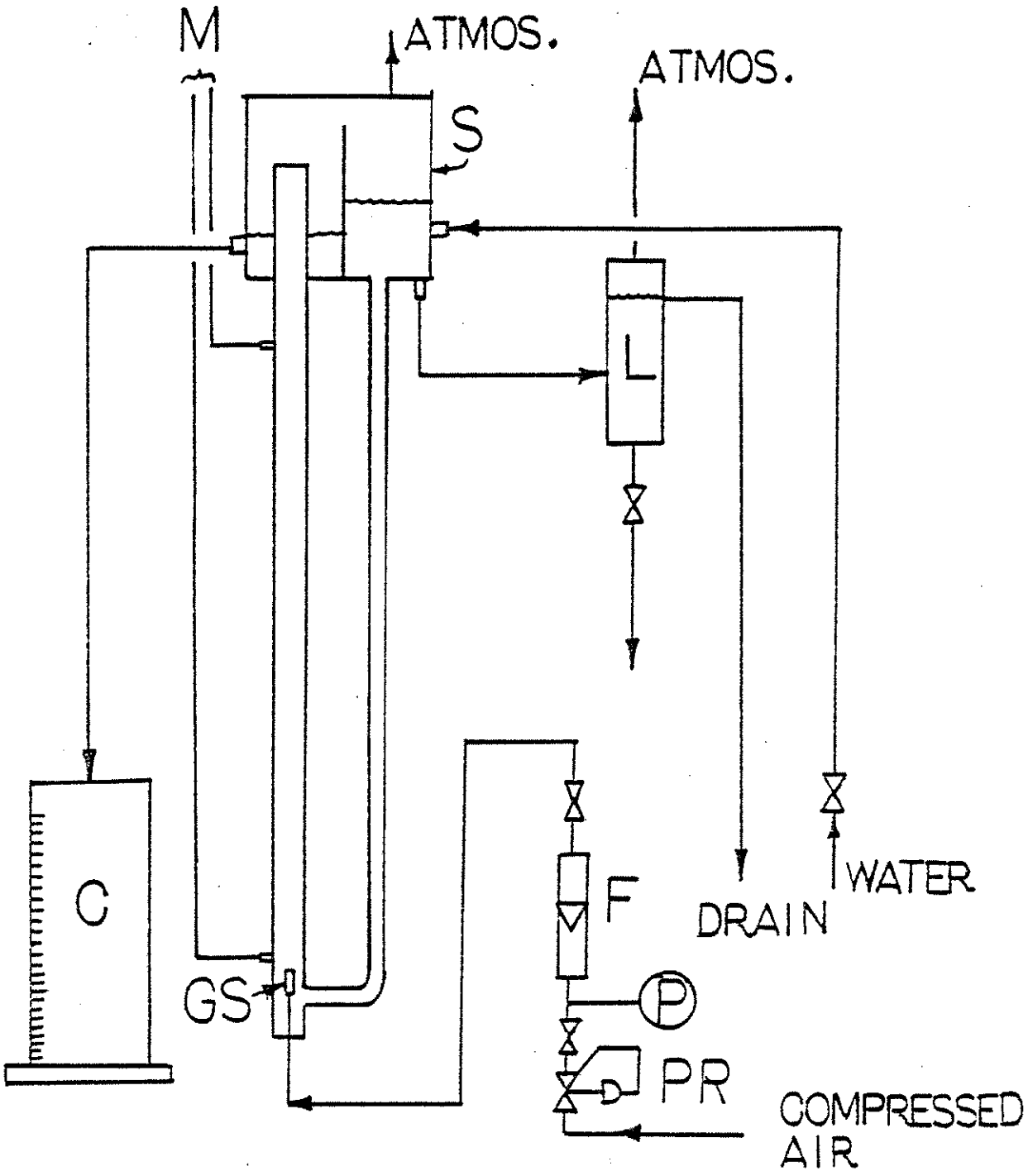

C : LIQ FLOW RATE MEAS. TANK S : SEPARATOR
GS : GAS SPARGER L : LEVEL CONTROL TANK
F : ROTAMETER M : MANOMETERS
P : PRESS. GA. PR : PRESS. REGULATOR

FIG 2 GAS LIFT APPARATUS

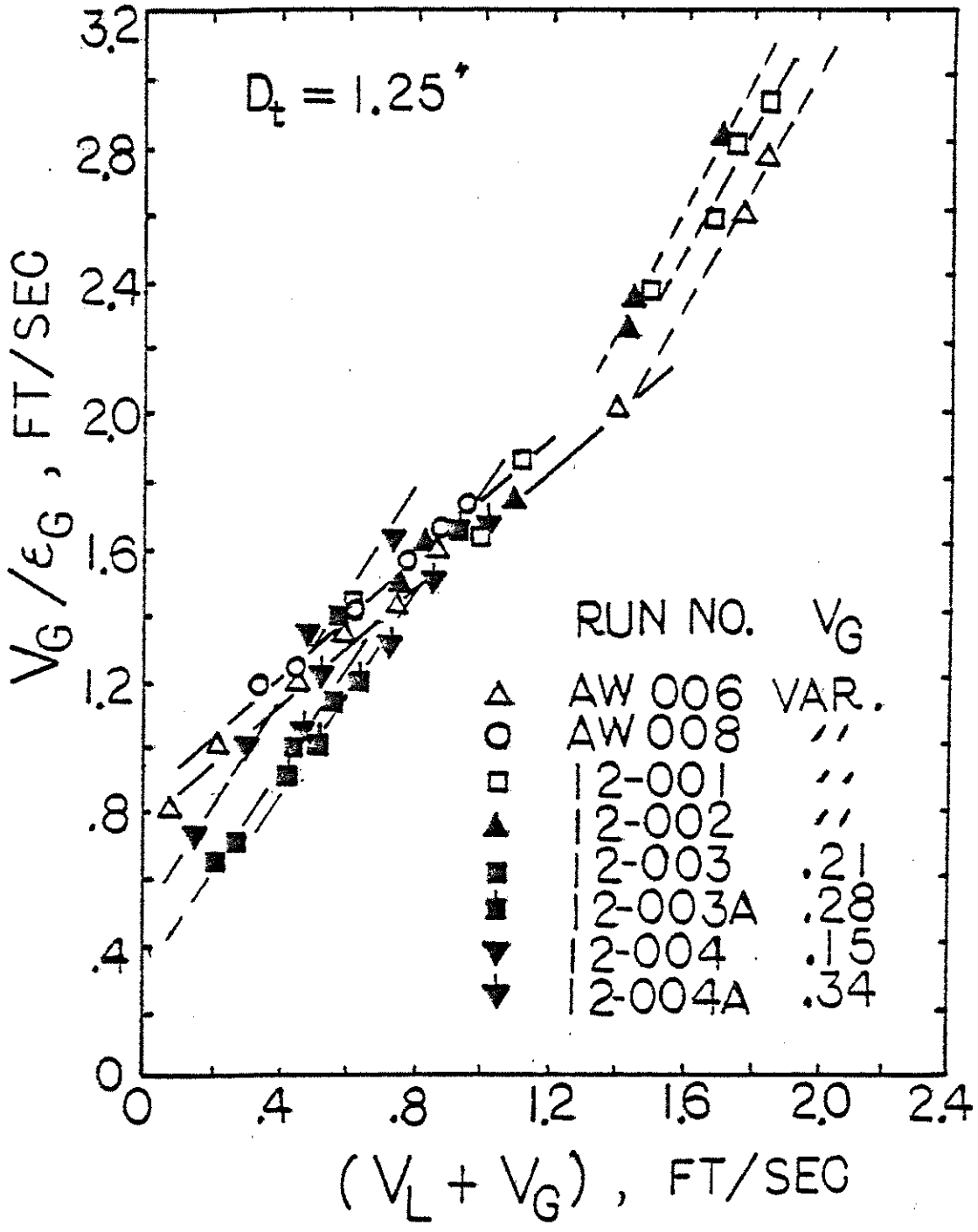

FIG 3 MEAN BUBBLE VELOCITY AS A FUNCTION OF TOTAL VELOCITY

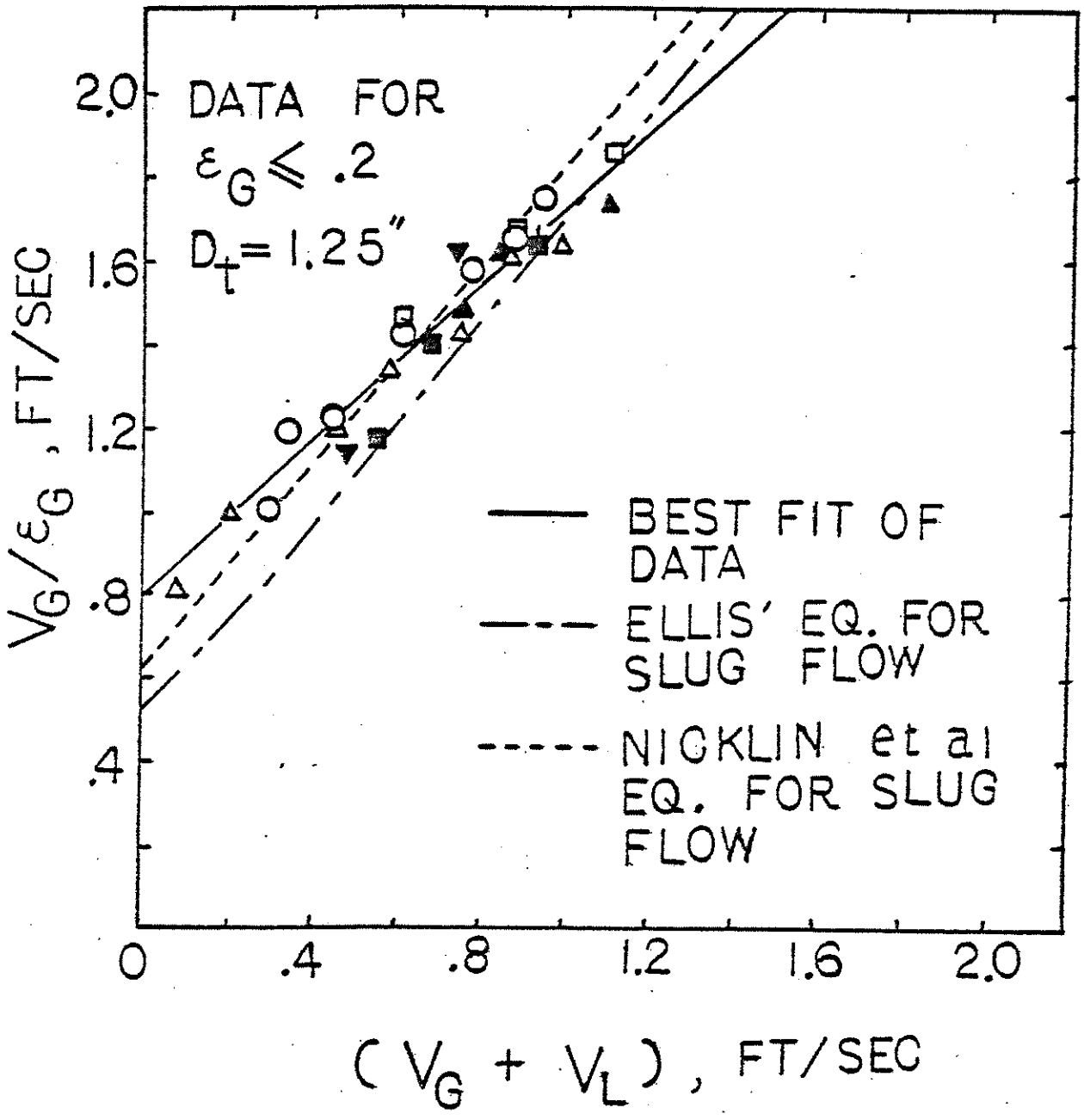

FIG 4 CORRELATION OF GAS HOLDUP

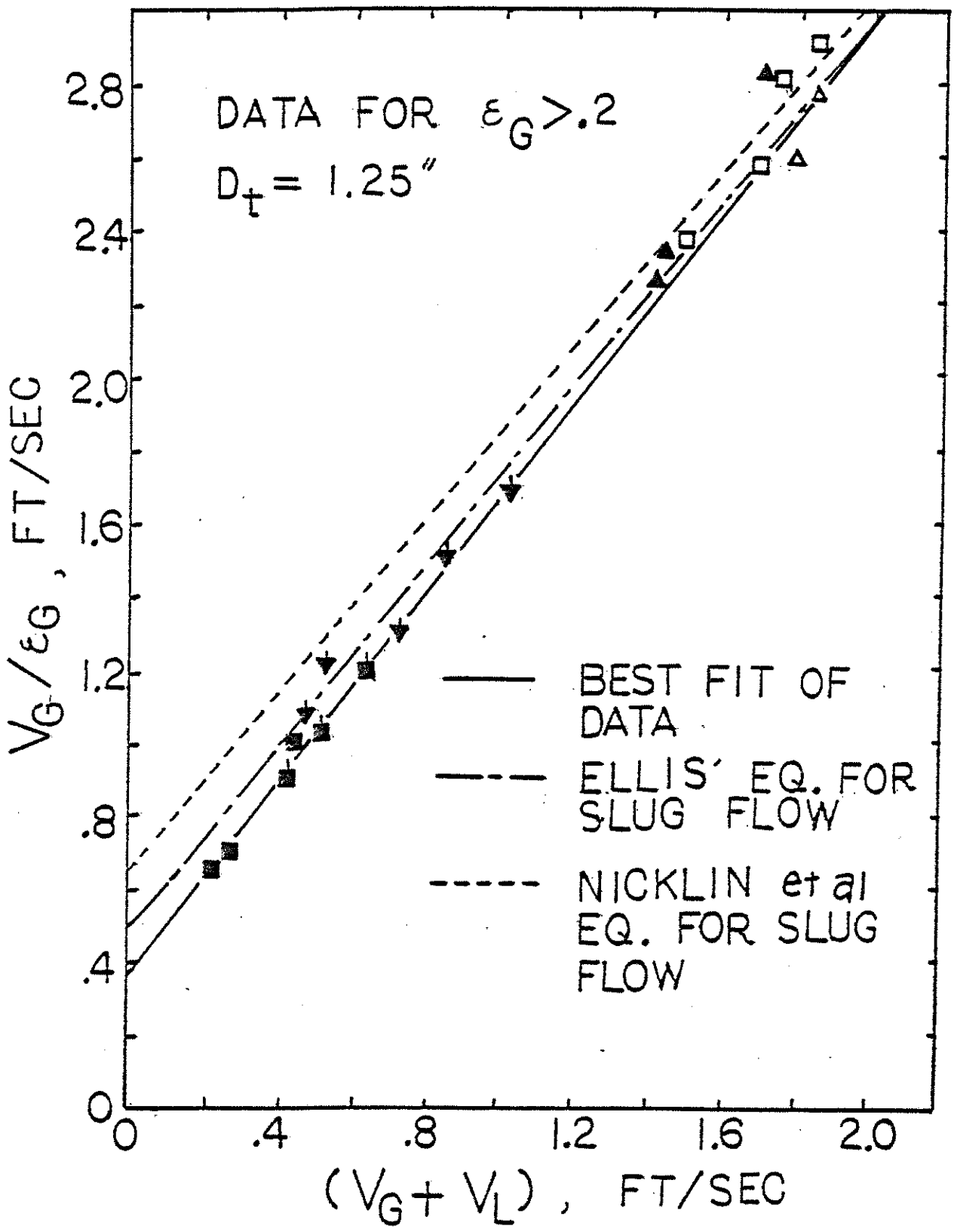

FIG 5 CORRELATION OF GAS HOLDUP

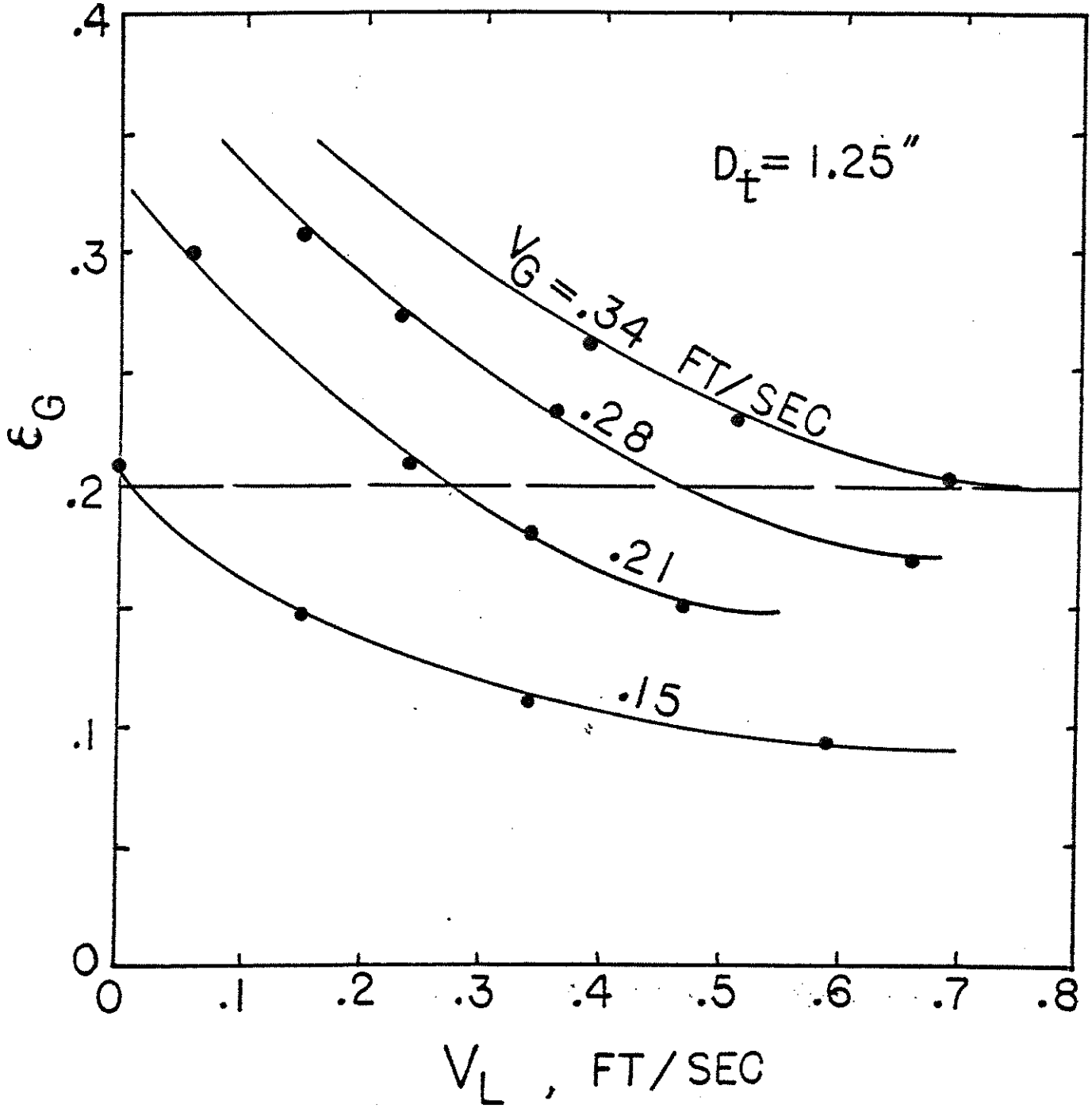

FIG 6 GAS HOLDUP AS A FUNCTION OF V_L AND V_G

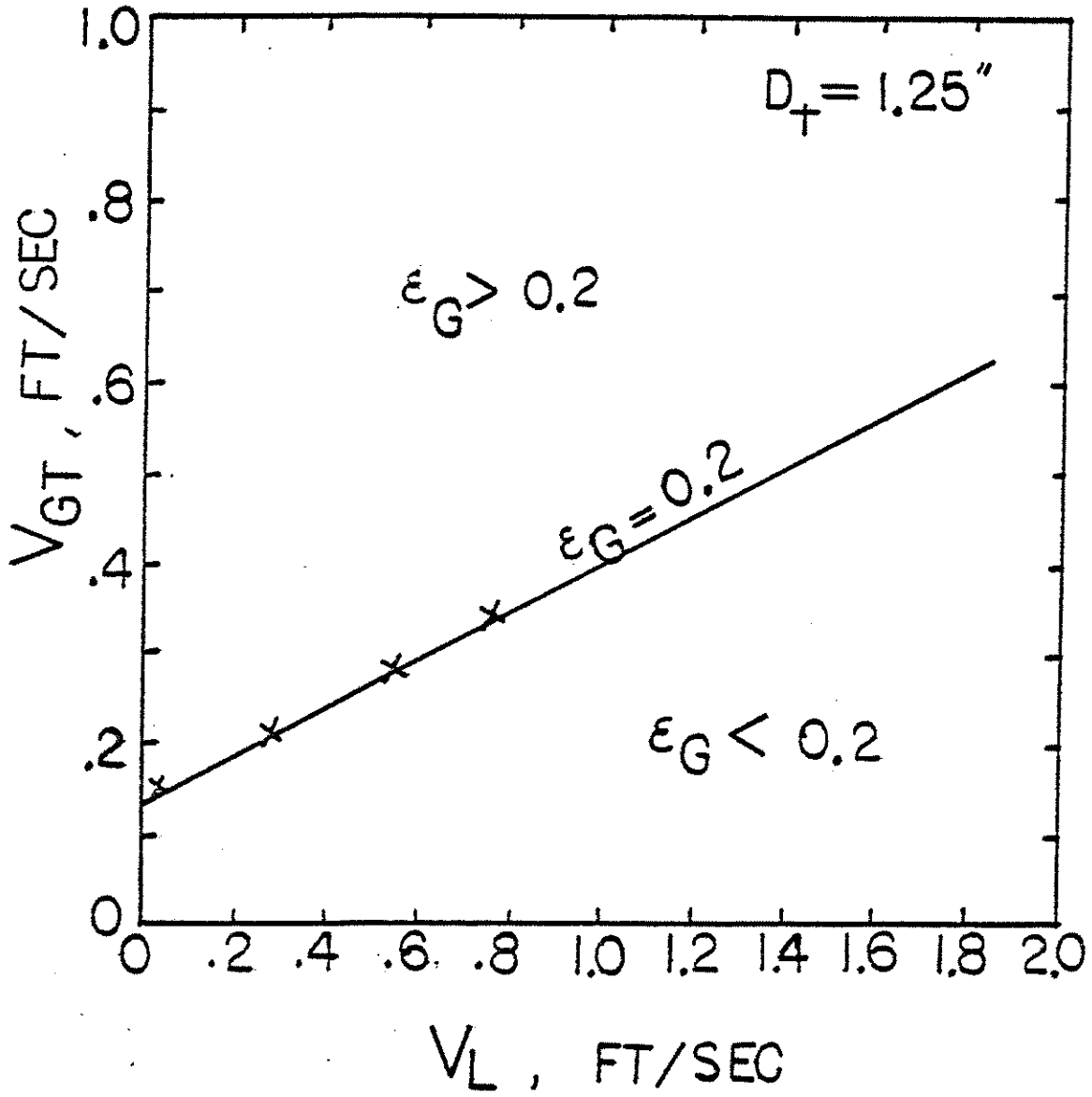

FIG 7 TRANSITION OF FLOW

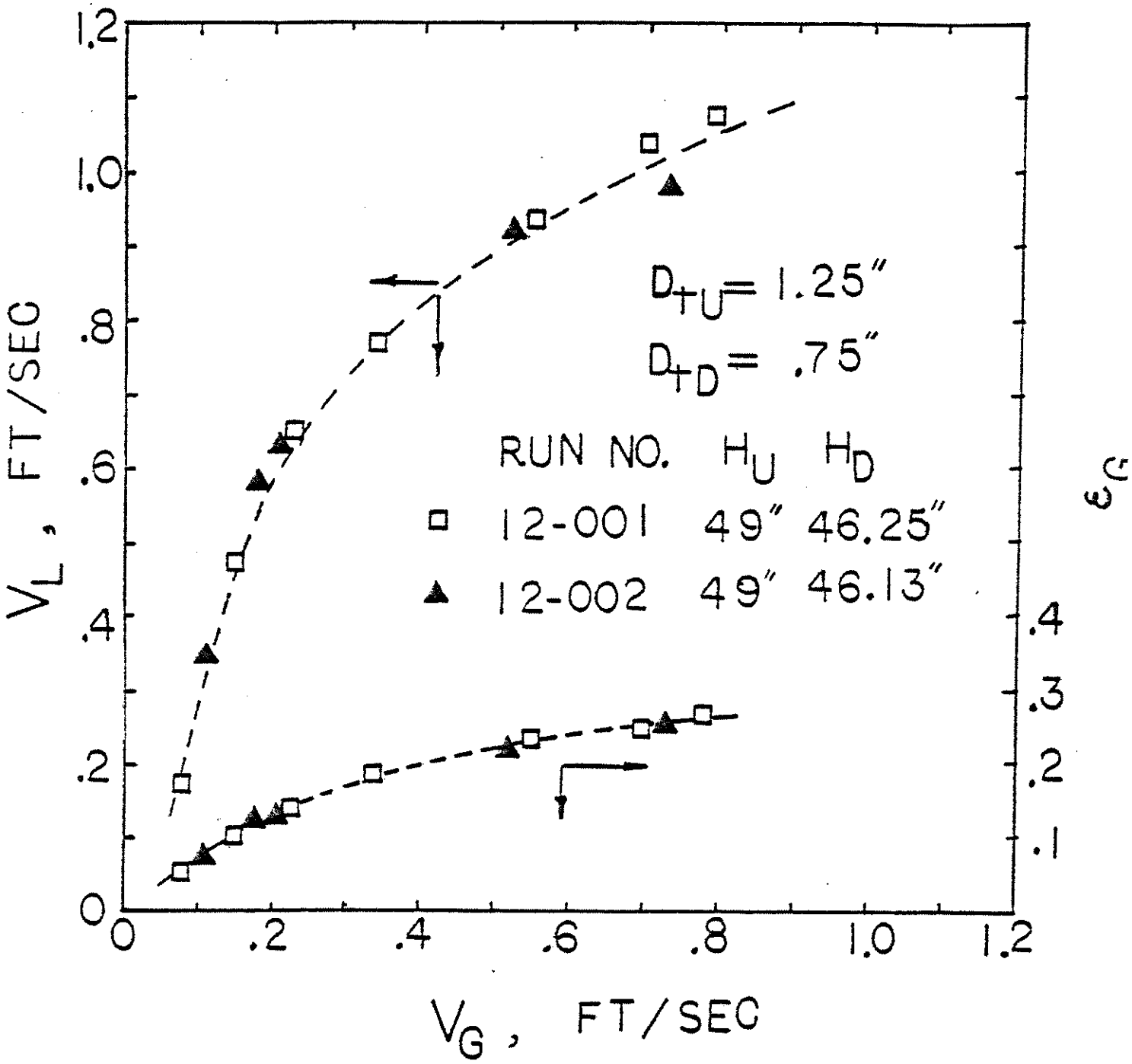

FIG 8 TYPICAL EXPERIMENTAL RESULTS OF GAS-LIFT APPARATUS

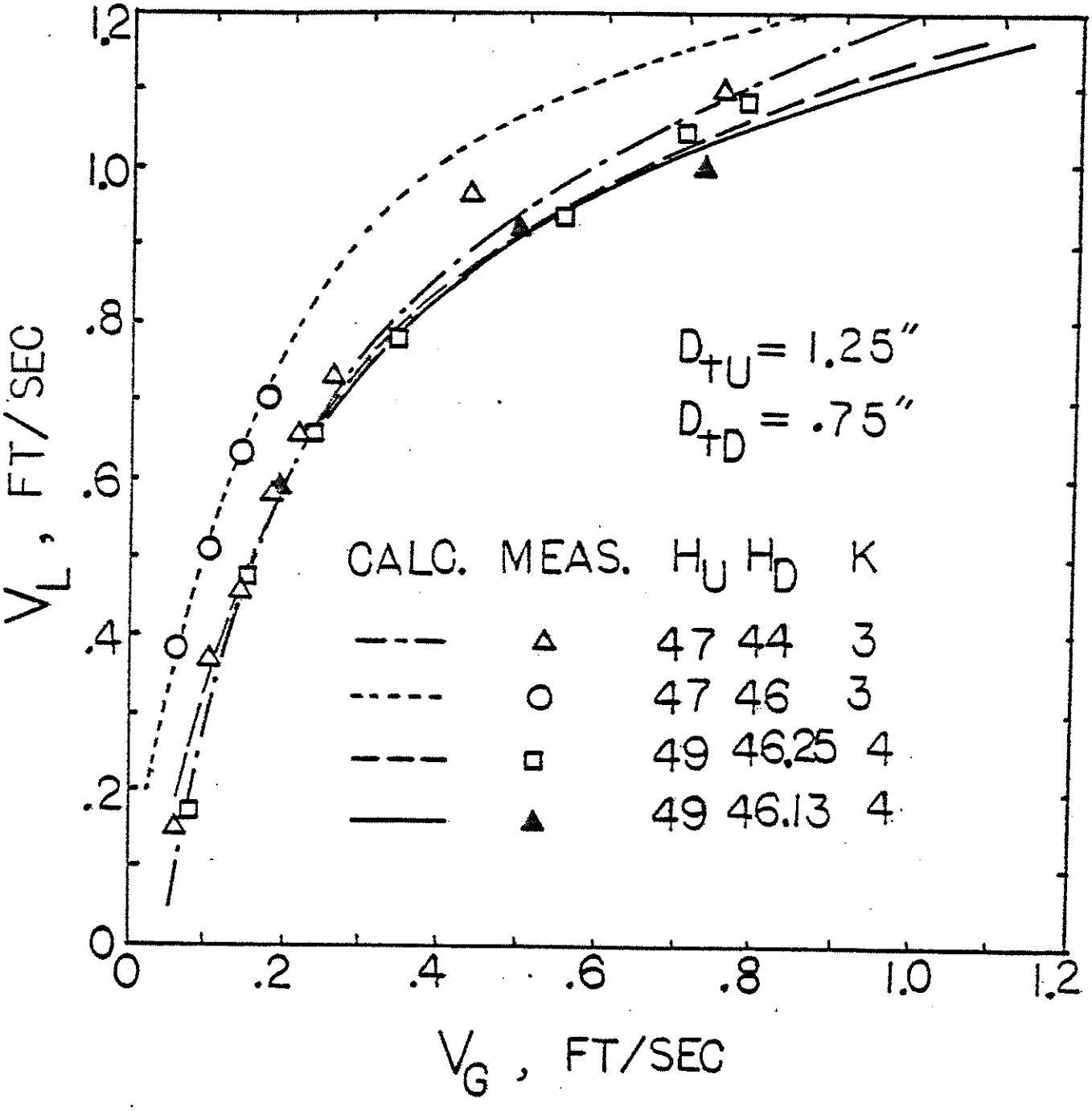

FIG 9 PREDICTION OF LIQUID RECIRCULATION RATES